Systems/Circuits

GnRH Neuron-Specific Ablation of $G\alpha_{q/11}$ Results in Only Partial Inactivation of the Neuroendocrine-Reproductive Axis in Both Male and Female Mice: *In Vivo* Evidence for Kiss1r-Coupled $G\alpha_{q/11}$-Independent GnRH Secretion

Andy V. Babwah,[1,2,3,4]* Víctor M. Navarro,[12] Maryse Ahow,[1,2,4†] Macarena Pampillo,[1,2,3†] Connor Nash,[6] Mehri Fayazi,[1,2,4] Michele Calder,[1,2,3] Adrienne Elbert,[1,2] Henryk F. Urbanski,[8,9,10,11] Nina Wettschureck,[7] Stefan Offermanns,[7] Rona S. Carroll,[12] Moshmi Bhattacharya,[4,5] Stuart A. Tobet,[6] and Ursula B. Kaiser[12]*

[1]The Children's Health Research Institute, Victoria Research Laboratories, London Ontario, N6C 2V5, Canada, [2]Lawson Health Research Institute, London, Ontario N6A 4V2, Canada, Departments of [3]Obstetrics and Gynaecology, [4]Physiology and Pharmacology, and [5]Oncology, University of Western Ontario, London, Ontario N6A 3K7, Canada, [6]Department of Biomedical Sciences, Colorado State University, Fort Collins, Colorado 80523, [7]Department of Pharmacology, Max Planck Institute for Heart and Lung Research, 61231 Bad Nauheim, Germany, [8]Divisions of [8]Neuroscience and [9]Reproductive and Developmental Sciences, Oregon National Primate Research Center, Beaverton, Oregon 97006, Departments of [10]Behavioral Neuroscience and [11]Physiology and Pharmacology, Oregon Health & Sciences University, Portland, Oregon 97239, and [12]Division of Endocrinology, Diabetes and Hypertension, Brigham and Women's Hospital and Harvard Medical School, Boston, Massachusetts 02115

The gonadotropin-releasing hormone (GnRH) is the master regulator of fertility and kisspeptin (KP) is a potent trigger of GnRH secretion from GnRH neurons. KP signals via KISS1R, a $G\alpha_{q/11}$-coupled receptor, and mice bearing a global deletion of *Kiss1r* (*Kiss1r*$^{-/-}$) or a GnRH neuron-specific deletion of *Kiss1r* (*Kiss1r*$^{d/d}$) display hypogonadotropic hypogonadism and infertility. KISS1R also signals via β-arrestin, and in mice lacking β-arrestin-1 or -2, KP-triggered GnRH secretion is significantly diminished. Based on these findings, we hypothesized that ablation of $G\alpha_{q/11}$ in GnRH neurons would diminish but not completely block KP-triggered GnRH secretion and that $G\alpha_{q/11}$-independent GnRH secretion would be sufficient to maintain fertility. To test this, *Gnaq* (encodes $G\alpha_q$) was selectively inactivated in the GnRH neurons of global *Gna11* (encodes $G\alpha_{11}$)-null mice by crossing *Gnrh-Cre* and *Gnaq*$^{fl/fl}$;*Gna11*$^{-/-}$ mice. Experimental *Gnaq*$^{fl/fl}$;*Gna11*$^{-/-}$;*Gnrh-Cre* (*Gnaq*$^{d/d}$) and control *Gnaq*$^{fl/fl}$;*Gna11*$^{-/-}$ (*Gnaq*$^{fl/fl}$) littermate mice were generated and subjected to reproductive profiling. This process revealed that testicular development and spermatogenesis, preputial separation, and anogenital distance in males and day of vaginal opening and of first estrus in females were significantly less affected in *Gnaq*$^{d/d}$ mice than in previously characterized *Kiss1r*$^{-/-}$ or *Kiss1r*$^{d/d}$ mice. Additionally, *Gnaq*$^{d/d}$ males were subfertile, and although *Gnaq*$^{d/d}$ females did not ovulate spontaneously, they responded efficiently to a single dose of gonadotropins. Finally, KP stimulation triggered a significant increase in gonadotropins and testosterone levels in *Gnaq*$^{d/d}$ mice. We therefore conclude that the milder reproductive phenotypes and maintained responsiveness to KP and gonadotropins reflect $G\alpha_{q/11}$-independent GnRH secretion and activation of the neuroendocrine-reproductive axis in *Gnaq*$^{d/d}$ mice.

Key words: β-arrestin; GnRH; GnRH secretion; Gq; KISS1R; kisspeptin

Significance Statement

The gonadotropin-releasing hormone (GnRH) is the master regulator of fertility. Over the last decade, several studies have established that the KISS1 receptor, KISS1R, is a potent trigger of GnRH secretion and inactivation of KISS1R on the GnRH neuron results in infertility. While KISS1R is best understood as a $G\alpha_{q/11}$-coupled receptor, we previously demonstrated that it could couple to and signal via non-$G\alpha_{q/11}$-coupled pathways. The present study confirms these findings and, more importantly, while it establishes $G\alpha_{q/11}$-coupled signaling as a major conduit of GnRH secretion, it also uncovers a significant role for non-$G\alpha_{q/11}$-coupled signaling in potentiating reproductive development and function. This study further suggests that by augmenting signaling via these pathways, GnRH secretion can be enhanced to treat some forms of infertility.

Introduction

The gonadotropin-releasing hormone (GnRH) is the master regulator of fertility. A large number of extrinsic and intrinsic signals acting through afferent systems converge upon GnRH neurons to regulate GnRH secretion. To receive and transmit these signals intracellularly, GnRH neurons express several receptors, of which the GPCRs represent a major class (Todman et al., 2005). Mice bearing a global deletion of the G-protein-coupled kisspeptin (KP) receptor, Kiss1r, or a GnRH neuron-specific deletion of Kiss1r display hypogonadotropic hypogonadism and are infertile, recapitulating phenotypes observed in human patients bearing *KISS1R*-inactivating mutations (Funes et al., 2003; Seminara et al., 2003; de Roux et al., 2003; Lapatto et al., 2007; Kirilov et al., 2013; Novaira et al., 2014). Together, these findings reveal that the GnRH neuronal-based kisspeptin/KISS1R signaling system is a potent trigger of GnRH secretion and thereby a major regulator of fertility.

Kiss1r was initially reported to signal via $G\alpha_{q/11}$ and thereby mediate GnRH secretion (Kotani et al., 2001; Muir et al., 2001; Ohtaki et al., 2001; Liu et al., 2008; Zhang et al., 2013). However, members of our group demonstrated that KISS1R also signals via β-arrestin (Pampillo et al., 2009; Szereszewski et al., 2010) and more recently reported that in mice lacking β-arrestin-1 or -2, KP54-triggered GnRH secretion was significantly diminished, as assessed indirectly by measuring serum gonadotropin levels (Ahow et al., 2014). Thus, we concluded that in the mouse, Kiss1r uses both $G\alpha_{q/11}$-dependent and -independent pathways (such as β-arrestin-1 or -2) to regulate GnRH secretion. These results are not surprising as we continue to better appreciate and understand the diversity and redundancy in signaling mechanisms in all cell types throughout the body. It is not known whether Kiss1r signals via $G\alpha_{q/11}$-dependent and -independent pathways in all Kiss1r-expressing GnRH neurons, or whether there are specific subpopulations of neurons in which a given pathway predominates. Nevertheless, based on our recent observations (Ahow et al., 2014), we hypothesize that in mice, loss of $G\alpha_{q/11}$ signaling in the GnRH neuron would significantly diminish GnRH secretion but not block it completely, and that $G\alpha_{q/11}$-independent GnRH secretion would be sufficient to maintain fertility.

To test this hypothesis, *Gnaq* (encodes $G\alpha_q$) was selectively inactivated in GnRH neurons of *Gna11* (encodes $G\alpha_{11}$)-null mice by crossing *Gnrh-Cre* and $Gnaq^{fl/fl}$;$Gna11^{-/-}$ mice to each other (Offermanns et al., 1998, Yoon et al., 2005). $G\alpha_q$ shares 88% amino acid identity with $G\alpha_{11}$ (Strathmann and Simon, 1990), and although the $Gnaq^{-/-}$ mouse displays phenotypic defects, suggesting that $G\alpha_{11}$ partially compensates for $G\alpha_q$ (Offermanns, 1997a,b), the $Gna11^{-/-}$ mouse is phenotypically normal, suggesting that $G\alpha_q$ compensates for $G\alpha_{11}$ (Offermanns et al., 1998). Consistent with these observations, the $Gnaq^{fl/fl}$;$Gna11^{-/-}$ mouse is phenotypically normal (Wettschureck et al., 2001). The well characterized *Gnrh-Cre* line is also phenotypically normal and efficiently targets hypothalamic GnRH neurons without disrupting gene expression in the pituitary, ovary, and testes (Yoon et al., 2005; Wintermantel et al., 2006; Kirilov et al., 2013). Recently, this line was used to inactivate GnRH neuron-specific *Kiss1r*, thereby generating mice that displayed hypogonadotropic hypogonadism and infertility (Kirilov et al., 2013).

Materials and Methods

Materials. KP54 (#SCP0186, human metastin 68–121), and Antide (catalog #A8802, GnRH antagonist) were purchased from Sigma. G-Protein Antagonist-2A (catalog #371780) was purchased from EMD Millipore. Unless stated, all other biochemical reagents were acquired from Sigma, Fisher Scientific, and VWR Scientific.

Animal husbandry and genotyping. Animal studies were approved by the University of Western Ontario Animal Care Committee according to guidelines established by the Canadian Council on Animal Care or by the Harvard Medical Area Standing Committee on the Use of Animals in Research and Teaching in the Harvard Medical School Center for Animal Resources and Comparative Medicine. The mice were maintained under a 12 h light/dark cycle and provided with standard rodent chow and water *ad libitum*.

Generation of $Gnaq^{fl/fl}$;$Gna11^{-/-}$;Gnrh-Cre ($Gnaq^{d/d}$) *experimental and* $Gnaq^{fl/fl}$;$Gna11^{-/-}$ ($Gnaq^{fl/fl}$) *littermate control mice.* The parental lines, $Gnaq^{fl/fl}$;$Gna11^{-/-}$ (Offermanns et al., 1998*Gnrh-Cre* (Yoon et al., 2005) mice, were generated as previously described; the *Gnrh-Cre* line was a generous gift from Dr. Catherine Dulac (Harvard University, Boston, MA). Parental lines, both maintained on the C57BL/6J genetic background, were crossed to each other to generate $Gnaq^{fl/+}$;$Gna11^{-/-}$;*Gnrh-Cre* F1 mice that were backcrossed to the parental line, $Gnaq^{fl/fl}$;$Gna11^{-/-}$, to generate an F2-segregating population of $Gnaq^{fl/fl}$;$Gna11^{-/-}$;*Gnrh-Cre* (experimental genotype bearing a GnRH neuron-specific deletion of *Gnaq* in the background of full-body deletion of *Gna11* and subsequently referred to as $Gnaq^{d/d}$) and $Gnaq^{fl/fl}$;$Gna11^{-/-}$ (control genotype subsequently referred to as $Gnaq^{fl/fl}$).

Mouse genotyping was performed by four PCRs using the following primers (presented 5′-3′): Gnaq forward GCATGCGTGTCCTTTATGTGAG and Gnaq reverse AGCTTAGTCTGGTGACAGAAGC, which generate a 600 and/or 700 bp product corresponding to the wild-type ($Gnaq^{+/+}$) and/or floxed allele ($Gnaq^{fl/fl}$), respectively (Dettlaff-Swiercz et al., 2005); Gna11-WT forward AGCATGCTGTAAGACCGTAG (Dettlaff-Swiercz et al., 2005) and Gna11-WT reverse GCCCCTTGTACAGATGGCAG, which generate an 820 bp product corresponding to the WT allele for $Gna11^{+/+}$; Gna11-KO forward CAGGGGTAGGTGATGATTGTGC and Gna11-WT reverse GACTAGTGAGACGTGCTACTTCC, which generate a 450 bp product corresponding to the deleted allele for $Gna11^{-/-}$ (Dettlaff-Swiercz et al., 2005); GnRH-Cre forward CTGGTGTAGCTGATGATCCG and GnRH-Cre reverse ATGGCTAATCGCCATCTTCC, which generate a 354 bp product corresponding to the Gnrh-Cre transgene (Druckenbrod and Epstein, 2005). When required to confirm the presence of GnRH neurons, reverse transcriptase (RT)-PCR was conducted to detect the expression of *Gnrh*. This was done using the following primers: Gnrh forward GCATTCTACTGCTGACTGTGTGTT and Gnrh reverse GTTCTGCCATTTGATCCACCT, which generate a 144 bp product (Luque et al., 2007). *Cre* expression was determined by RT-PCR using primers Cre forward GCATTACCGGTCGATGCAACGAGTGATGAG and Cre reverse GAG

Received Jan. 6, 2015; revised July 16, 2015; accepted Aug. 11, 2015.

Author contributions: A.V.B., V.M.N., C.N., R.S.C., M.B., S.A.T., and U.B.K. designed research; A.V.B., V.M.N., M.A., M.P., C.N., M.F., M.C., A.E., and R.S.C. performed research; H.F.U., N.W., S.O., M.B., S.A.T., and U.B.K. contributed unpublished reagents/analytic tools; A.V.B., V.M.N., M.A., M.P., C.N., M.F., M.C., A.E., H.F.U., N.W., S.O., R.S.C., M.B., S.A.T., and U.B.K. analyzed data; A.V.B., V.M.N., M.B., and U.B.K. wrote the paper.

The authors were supported by grants from the Natural Sciences and Engineering Research Council of Canada (NSERC) RGPIN/327334-2011 (A.V.B.); the Canadian Institutes of Health Reserach (CIHR) MOP107972 (M.B.); CIHR New Investigator's Award and the Early Researcher Award (ERA) from the Ministry of Research and Innovation, Ontario, Canada (A.V.B., M.B.); National Institutes of Health Grant OD-011092 (H.F.U.); National Institute of Child Health and Human Development (NICHD) Grant K99HD071970 and the Charles H. Hood Foundation Award for Child's Health (V.M.N.); and the Eunice Kennedy Shriver National Institute of Child Health and Human Development through cooperative agreement U54 HD028138 as part of the Specialized Cooperative Centers Program in Reproduction and Infertility Research grants from the National Institutes of Health and NICHD Grant R01 HD019938 (U.B.K.).

The authors declare no competing financial interests.

*A.V.B. and U.B.K. are co-senior authors.

†M.A. and M.P. contributed equally to this work.

Correspondence should be addressed to Dr. Andy V. Babwah, Children's Health Research Institute, Victoria Research Laboratories, A4-140, 800 Commissioners Road East, London, ON N6C 2V5, Canada. E-mail: ababwah@uwo.ca.

DOI:10.1523/JNEUROSCI.0041-15.2015

 0270-6474/15/3512904-14$15.00/0

TGAACGAACCTGGTCGAAATCAGTGCG, which generate a 408 bp product (White et al., 2007).

Developmental characterization of Gnrh-Cre *expression.* Although *Cre* expression was extensively characterized in the adult *Gnrh-Cre* mouse (Yoon et al., 2005; Wintermantel et al., 2006; Kirilov et al., 2013), our goal was to determine how early in development *Cre* was expressed. To do so, the *Gnrh-Cre* mouse was crossed to the *ROSA26-loxP-stop-loxP-GFP* reporter mouse (Mao et al., 2001). The *ROSA26-loxP-stop-loxP-GFP* reporter line (catalog #004077) was purchased from The Jackson Laboratory. The resulting progeny of genotype *ROSA26-loxP-stop-loxP-GFP*; *Gnrh-Cre* were killed at embryonic day 18 (E18) and postnatal day 7 (P7), P14, and P21. Mice were transcardially perfused with 4% paraformaldehyde (PFA), and brains were removed and postfixed for 3 h in 8% PFA, then infiltrated with 30% sucrose. Coronal sections, 30 μm thick, were cut on a Leica freezing microtome and blocked in 10% normal donkey serum for 1 h at room temperature and incubated overnight at 4°C in the rabbit anti-GnRH primary polyclonal antibody, HU60 (Urbanski et al., 1990). The primary antibody was used at a concentration of 1:1000. After this, tissue sections were washed in PBS and blocked in 10% normal donkey serum, then incubated at room temperature in secondary antibody for 2 h (Alexa Fluor 568, 1:2000 goat anti-rabbit; Life Technologies Inc.). Sections were subsequently stained with Hoechst (Life Technologies Inc.), 1:10,000 for 3 min, to detect nuclei and then washed in PBS and mounted on positively charged microscope slides and allowed to dry before being coverslipped with Immuno-Mount (Fisher Scientific). Sections were viewed and images captured using an Olympus Fluoview 1000 laser scanning confocal microscope. Colocalization studies were performed using multiple-excitation (405, 488, 559) and emission (bandpass 425–475, 500–545 nm and 575–675 nm for Hoechst, GFP, and Alexa Fluor 568, respectively) filter sets. Multicolor images were acquired in the sequential acquisition mode to avoid cross-excitation. Ten consecutive coronal sections per brain, spanning the rostral-caudal hypothalamic axis, were analyzed by confocal microscopy where neuronal soma were scored for green (GFP) and red (GnRH) signals.

Immunohistochemical analysis of GnRH neurons. Mouse brains were collected and processed as previously described (Ahow et al., 2014) and cut into 50-μm-thick coronal sections. Sections were blocked in 5% normal goat serum for 1 h at 4°C and incubated over two nights at 4°C in primary anti-GnRH polyclonal antibody (EL14, 1:5000 dilution; Ellinwood et al., 1985). Next, sections were incubated for 2 h at room temperature in a biotin-conjugated donkey anti-rabbit secondary antibody (Jackson ImmunoResearch) that was used at 1:2500. Secondary antibody labeling was amplified using a Vectastain ABC Elite kit (Vector Laboratories), and polymerized reaction product was created using DAB/Ni as substrate, as previously described (Ahow et al., 2014). Mounted sections were viewed and images were captured using an Olympus BH2 microscope with an Insight QE digital camera with Spot Advanced Software. Coronal brain slices along the rostral-caudal axis were ordered and aligned relative to the organum vasculosum of the lamina terminalis (OVLT), and an investigator blind to genotype manually counted GnRH neuronal cell bodies using a 40× objective (Gill et al., 2008). The effect of genotype on the number and location of GnRH neurons was determined by two-way ANOVA as a repeated measure using SPSS software. Values are reported as mean ± SEM and $p < 0.05$ was considered statistically significant.

Pubertal onset, determination of first estrus, estrous staging, and fertility assessment. Mice were genotyped and weaned by 3 weeks of age. For both females and males, body weight (grams) was recorded weekly. Females and males were also examined daily from 2 weeks of age until the day of vaginal opening and preputial separation, respectively. Preputial separation was assessed by applying gentle pressure to manually retract the prepuce (Gaytan et al., 1988). For males, anogenital distance (millimeters) was recorded every 3–7 d. First estrus and estrous staging (proestrus, estrus, or metestrus/diestrus) were based visually on the relative amounts of cornified epithelial, nucleated epithelial, and polymorphonuclear leukocytes present in vaginal smears (Caligioni, 2009). Smears were collected daily for 17 d between 8:00 and 10:00 A.M. in 8- to 11-week-old females and again for another 17 d in the same females at 13–16 weeks of age. The average number of times $Gnaq^{d/d}$ mice entered estrus during the two 17 d periods was compared with $Gnaq^{fl/fl}$ littermates using unpaired two-tailed *t* tests. All phenotyping experiments were done without concurrent knowledge of the genotype. To assess fertility, 7-week-old male and female $Gnaq^{d/d}$ mice were placed in a cage with a WT mouse of the opposite sex and proven fertile, and females were regularly observed for evidence of pregnancy over a period of 21 d.

Anatomical and histological analyses of reproductive organs. All mice used were 8–16 weeks of age and previously untreated and unmated. Ovaries and uteri were taken from females in the metestrus stage since this stage is easily identified by vaginal cytology, and testes were taken from the males. Total body weight (grams), tissue appearance, and fresh weight of female reproductive tracts and male testes (milligrams) were noted. Tissues were fixed in 4% PFA-PBS overnight, then dehydrated in 70% ethanol for 24 h before paraffin embedding, sectioning (5 μm thick), and staining with hematoxylin and eosin. Ovarian and testicular sections were examined and photographed with an Aperio ScanScope XT in conjunction with ImageScope software.

KP54 and Antide (GnRH-antagonist) treatment studies. To avoid interference by cycle-dependent leuteinizing hormone (LH) surges with kisspeptin-induced LH secretion, 7-week-old virgin $Gnaq^{d/d}$ and $Gnaq^{fl/fl}$ female mice were bilaterally ovariectomized (Ström et al., 2012). Ovariectomized females, 14 d postsurgery, and intact males 9 weeks of age were administered a single intraperitoneal injection of 100 μl of PBS (vehicle) or 100 nmol KP54/kg body weight in a final volume of 100 μl (Ahow et al., 2014). One hour later, mice were anesthetized by CO_2 exposure and blood was collected by cardiac puncture. In a separate cohort of 9-week-old ovariectomized females and intact males, mice received two 100 μl subcutaneous injections of the GnRH antagonist, Antide (1.25 μg/g body weight dissolved in sterile saline). Antide was administered at 24 and 1 h before intraperitoneal injection of 100 μl of saline vehicle or 100 μl of 0.1 nmol KP54/g body weight (Ahow et al., 2014). Blood was collected by cardiac puncture 1 h after the final injection.

G-protein antagonist 2A treatment studies. Experiments were conducted on intact adult $Gnaq^{d/d}$ males. G-protein antagonist 2A (GP-2A) and KP54 were administered centrally through intracerebroventricular injections into the lateral cerebral ventricle; the site of the injection was 1 mm posterior and 1.2 mm lateral to bregma. Mice were injected with KP54 (100 pmol/5 μl) or the $G\alpha_q$ inhibitor, GP-2A (5 nmol/5 μl), and blood was collected by retro-orbital bleeding 30 min after injection. For the GP-2A + KP54 group, mice were injected with GP-2A first, then with KP54 30 min later, and then blood was collected 30 min after KP54 injection.

Serum hormone assays. In the KP54 and Antide treatment studies, in which blood was collected by cardiac puncture, blood was processed and serum was analyzed for follicle-stimulating hormone (FSH) and LH by the Endocrine Technology and Support Laboratory, Oregon National Primate Research Center (Beaverton, OR) as previously described (Pau et al., 1986; Ahow et al., 2014; Calder et al., 2014). The detection limits of the FSH and LH assays were 0.1–0.2 ng/ml. The intra- and interassay variations were <8 and 12%, respectively. In addition to FSH and LH, mouse serum testosterone was measured as described previously (Rasmussen et al., 1984). Briefly, samples were extracted in ether and analyzed by specific testosterone RIA using tritium-labeled testosterone as the trace and the Holly Hills Lot A-1 testosterone antibody. The sensitivity was 5 pg/tube and the intra- and interassay variations were <10% and 15%, respectively. Data were analyzed by Student's *t* test, where $p < 0.05$ was considered statistically significant. In the GP-2A and L-NAME studies, where blood was collected by retro-orbital bleeding, blood was processed and serum LH levels were measured using a Milliplex MAP immunoassay (Mouse Pituitary panel, Millipore) in the Luminex 200 (Singh et al., 2009; Martin et al., 2014; Navarro et al., 2015). The minimum detectable concentration for LH was 2.4 pg/ml. The intra-assay coefficient of variation was <8.78%. Data were analyzed by one-way ANOVA followed by a Tukey *post hoc* test where $p < 0.05$ was considered statistically significant.

Quantitative real-time RT-PCR studies. Gene expression was determined in total RNA prepared from the entire hypothalamus, pituitary, ovary, and testes. Freshly harvested tissues were collected in RNAlater

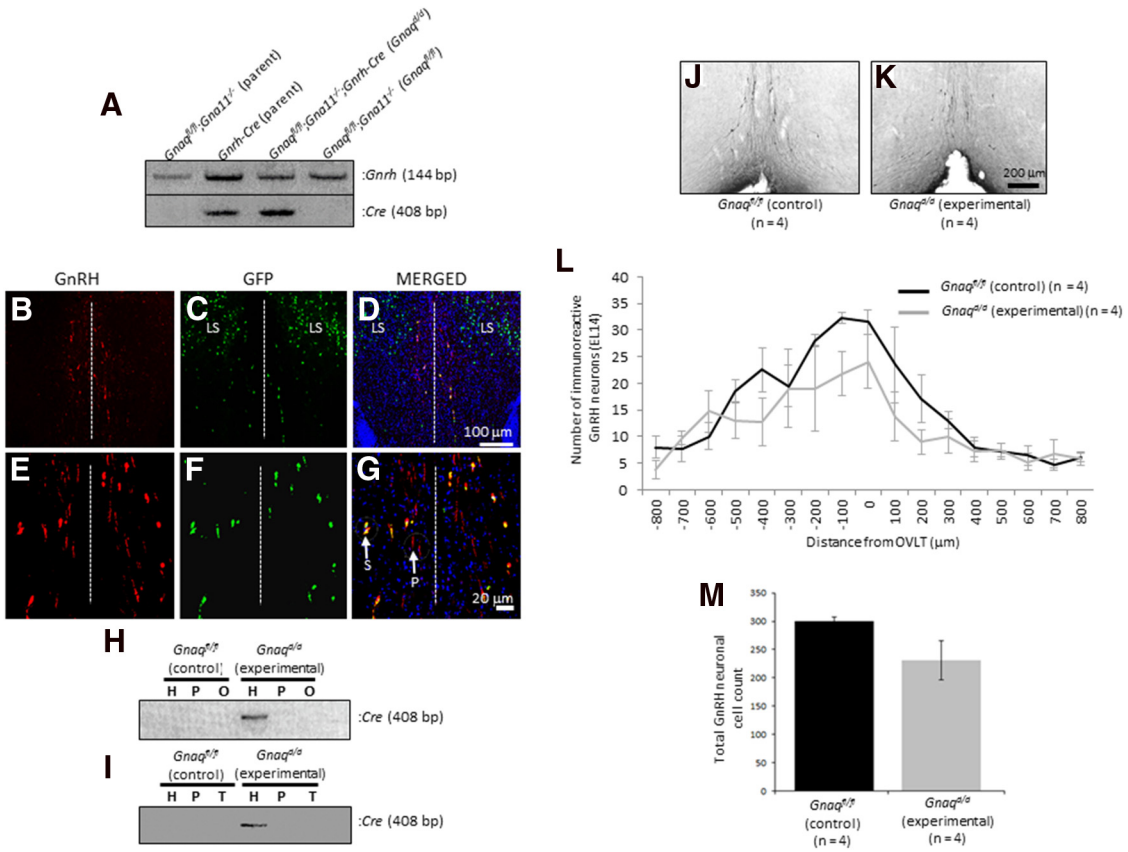

Figure 1. Generation of *Gnaq*$^{fl/fl}$;*Gna11* $^{-/-}$;*Gnrh-Cre* (*Gnaq*$^{d/d}$) experimental and *Gnaq*$^{fl/fl}$;*Gna11* $^{-/-}$ (*Gnaq*$^{fl/fl}$) littermate control mice. ***A***, RT-PCR analysis of gene expression reveals that the hypothalamus of the *Gnrh-Cre* parental line, as confirmed by *Gnrh* expression, expresses *Cre* and that among the F2-segregating population, the experimental genotype *Gnaq*$^{fl/fl}$;*Gna11* $^{-/-}$;*Gnrh-Cre* (subsequently designated *Gnaq*$^{d/d}$) expresses *Cre*, whereas control littermates *Gnaq*$^{fl/fl}$;*Gna11* $^{-/-}$ (subsequently designated *Gnaq*$^{fl/fl}$) do not. ***B–D***, Immunofluorescence analysis of the E18 hypothalamus from progeny derived from a cross between the *Gnrh-Cre* and *ROSA26-loxP-stop-loxP-GFP* reporter line reveals that GFP is expressed in neurons localized to the LS and periventricular region and that only neurons in the latter region coexpress GnRH. ***E–G***, Immunofluorescence analysis of neurons that coexpress GFP and GnRH in the periventricular region show that the expression of GFP is restricted to the soma (S), whereas GnRH is detected in both the soma and processes (P) of the GnRH neurons. The dashed white line indicates the midline of the coronal slice. ***H***, ***I***, RT-PCR analysis of *Gnrh-Cre* expression in the hypothalamus (H), pituitary (P), ovaries (O), and testes (T) of experimental *Gnaq*$^{d/d}$ mice. ***J***, ***K***, Photomicrographs of coronal brain sections at the level of the OVLT from 8-week-old *Gnaq*$^{fl/fl}$ and *Gnaq*$^{d/d}$ mice. In photomicrographs, GnRH neurons were revealed in the brain slices by immunohistochemistry using the EL14 antibody, and the OVLT was used as a neuroanatomical reference point for rostral to caudal alignment of coronal sections. ***L***, Histogram displays the rostral-caudal distribution of GnRH-immunoreactive neurons from *Gnaq*$^{fl/fl}$ and *Gnaq*$^{d/d}$ mice aligned at the OVLT. Plot represents average GnRH-immunoreactive neurons per 50 μm coronal section. ***M***, Total number of GnRH-immunoreactive neurons identified in *Gnaq*$^{fl/fl}$ and *Gnaq*$^{d/d}$ mice with the EL14 antibody. Error bars represent SEM.

(Life Technologies Inc.) and RNA was isolated using the Qiagen RNeasy mini kit according to the manufacturer's instructions. RNA concentration was determined by optical density (260/280 nm) on an ND-1000 spectrophotometer (NanoDrop). RNA (1.0 μg) was reverse-transcribed using SuperScript II (Invitrogen). Reactions were performed according to the manufacturer's protocol using random hexamer primers (GE Healthcare). Quantitative real-time PCR was performed in duplicate for each sample, for a total of three independent times, using IQ SYBR Green Master Mix (Bio-Rad Laboratories). To determine PCR efficiency, a ten-fold serial dilution of cDNA was performed as described previously (Wong and Medrano, 2005). Gene expression was normalized to *Actb* expression and presented as relative expression using the Pfaffl method (Pfaffl, 2001). Expression of the following genes was quantified using the following primers (presented 5′-3′). *Kiss1*: Kiss1 forward, AGCTGCTGCTTCTCCTCTGT, and Kiss1 reverse, AGGCTTGCTCTCTGCATACC, which generate a 140 bp product; Kiss1r forward, GCCACAGACGTCACTTTCCTAC, and Kiss1r reverse, CGGGAACACAGTCACATACCA, which generate a 186 bp product; *Gnrh1*: Gnrh1 forward, CCTGGGGGAAAGAGAAACACT, and Gnrh1 reverse, TCACAAGCCTCAGGGTCAATG, which generate a 246 bp product; *Gnrhr1*: Gnrhr1 forward, GCTCTCAAGGATGAAGGTGCTT, and Gnrhr1 reverse, CCAGGCTAATCACCACCATCAT, which generate a 197 bp product; *Fshb*: Fshb forward, AGAGAAGGAAGAGTGCCGTTTCTG, and Fshb reverse, ACATACTTTCTGGGTATTGGGCCG, which generate a 118 bp product; and *Lhb*: Lhb forward, TGTCCTAGCATGGTCCGAGT, and Lhb reverse, AGGAAAGGAGACTATGGGGTCTA, which generate a 138 bp product.

Superovulation of female Gnaq$^{d/d}$ *mice and isolation and characterization of preimplantation embryos.* Female *Gnaq*$^{d/d}$ mice, 6–8 weeks old, were administered 7.5 IU pregnant mare serum gonadotrophin (Folligon; Intervet), i.p., followed 48 h later by 7.5 IU human chorionic gonadotropin (hCG; Chorulon; Intervet), i.p. Immediately after the hCG injection, mice were mated to WT males of proven fertility. Day of mating is defined as D0. Only females that showed a copulatory plug (evidence of successful mating) on the morning of D1 were studied further. Preimplantation embryos were collected on D4 from the uterus for characterizing preimplantation embryonic development (Calder et al., 2014). Embryos were flushed from the reproductive tract using M2 medium (Sigma).

Results

Generation of *Gnaq*$^{fl/fl}$;Gna11$^{-/-}$;*Gnrh-Cre* (*Gnaq*$^{d/d}$) experimental and *Gnaq*$^{fl/fl}$;*Gna11*$^{-/-}$ (*Gnaq*$^{fl/fl}$) littermate control mice

To determine the role of $G\alpha_{q/11}$ signaling in regulating reproductive maturation at the level of the GnRH neuron, *Gnaq* was selectively inactivated in the GnRH neurons of *Gna11*-null mice by

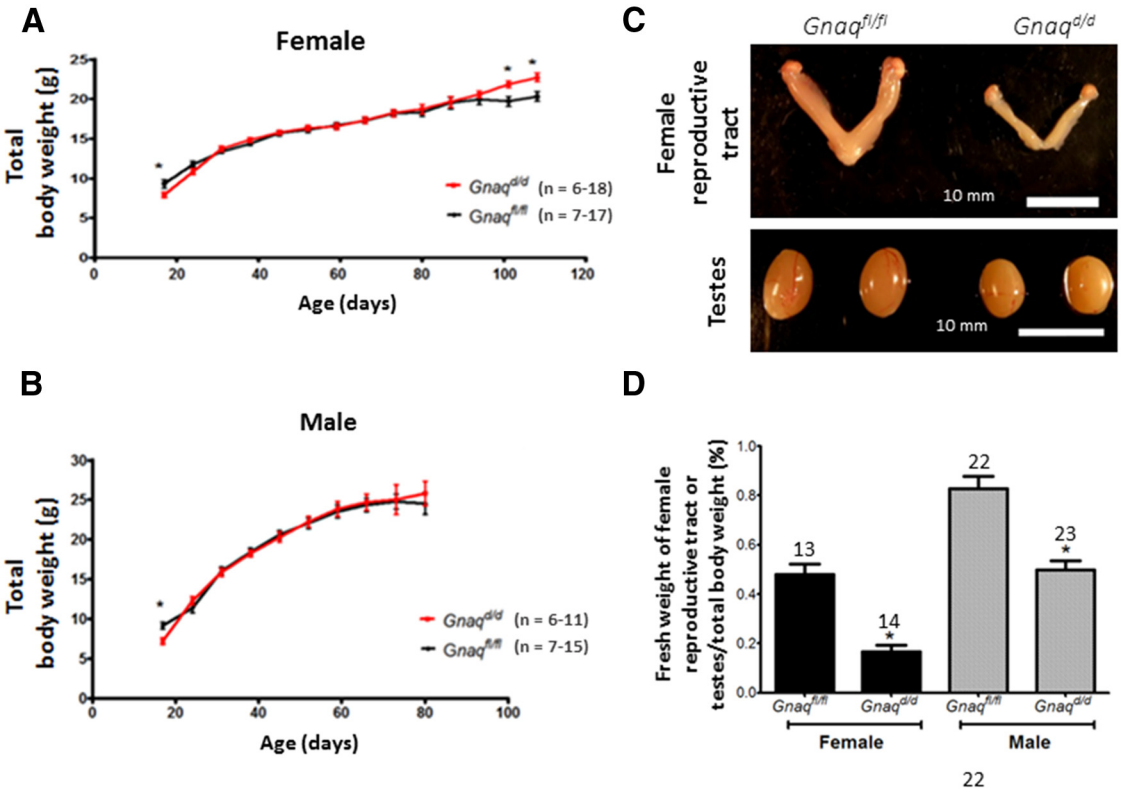

Figure 2. Maturation of *Gnaq*$^{fl/fl}$ and *Gnaq*$^{d/d}$ mice. ***A***, ***B***, Total body weight development in female (***A***) and male (***B***) *Gnaq*$^{fl/fl}$ and *Gnaq*$^{d/d}$ mice. ***C***, Gross anatomy of the female reproductive tract and male testes of *Gnaq*$^{fl/fl}$ and *Gnaq*$^{d/d}$ mice. Reproductive tracts and testes were taken from unmated and untreated 8- to 16-week-old mice. Females were in metestrus. ***D***, Bar chart illustrates the ratio of the fresh weight of the female reproductive tract or testes to total body weight. Error bars represent SEM. *$p < 0.05$, significant difference .

mating the *Gnrh-Cre* and *Gnaq*$^{fl/fl}$;*Gna11*$^{-/-}$ mouse to each other (Fig. 1*A*). Neither parental line shows any evidence of reproductive abnormalities compared with control littermates (Offermanns et al., 1998; Yoon et al., 2005). Although the *Gnrh-Cre* adult mouse was extensively characterized (Yoon et al., 2005; Wintermantel et al., 2006; Kirilov et al., 2013), our goal in the current study was to determine how early in development *Cre* was expressed. To do so, the *Gnrh-Cre* mouse was crossed to the *ROSA26-loxP-stop-loxP-GFP* reporter mouse (Mao et al., 2001) and the number of GnRH neurons (Fig. 1*B*,*E*) that expressed GFP in the E18 and P7, P14, and P21 hypothalamus was quantified (Fig. 1*C*,*D*,*F*,*G*; only representative E18 hypothalamus is shown). Results indicate that at all ages recombination of the stop codon occurred in >98% of all detectable GnRH neurons, a value consistent with that reported by others (Yoon et al., 2005; Wintermantel et al., 2006; Kirilov et al., 2013). In addition to observing Cre recombinase activity in GnRH neurons localized to the periventricular zone of the rostral hypothalamus, activity was also observed in the lateral septum (LS; (Fig. 1*C*,*D*). Cre activity in the LS was previously described by others in the GnRH-Cre mouse line used in this study (Yoon et al., 2005; Kirilov et al., 2013), as well as in at least one other independently generated line (Wolfe et al., 2008). These authors described the presence of a group of neurons in the LS that express Cre but not GnRH. It was reported that the LS is a site where GnRH is expressed transiently in the early postnatal period in the mouse brain (Skynner et al., 1999; Kirilov et al., 2013).

Next, *Cre* expression was assessed along the hypothalamic–pituitary–gonadal (HPG) axis of female and male mice, and results revealed that *Cre* expression was restricted to the hypothalamus and not detected in the pituitary and gonads of experimental *Gnaq*$^{d/d}$ mice (Fig. 1*F*,*G*). Overall, these results suggest that since *Cre* is expressed early in development, *Gnaq*$^{d/d}$ mice can be used to study the effect of an absence of $G\alpha_{q/11}$ signaling on reproductive maturation; furthermore, since *Cre* expression was restricted to GnRH neurons, any observed reproductive phenotypes would be the result of a loss of $G\alpha_{q/11}$ signaling in the GnRH neurons only.

To assess the functional effects of loss of $G\alpha_{q/11}$ signaling on GnRH secretion, it was important to first determine whether inactivation of *Gnaq* affected the size and distribution of the hypothalamic GnRH neuronal population in the anterior hypothalamus. Therefore, the number and location of the adult GnRH cell population were analyzed by comparing 8-week-old *Gnaq*$^{d/d}$ to *Gnaq*$^{fl/fl}$ male littermates. Representative coronal images from sections at the level of the OVLT are shown (Fig. 1*H*,*I*). The mean number of GnRH-immunoreactive neurons in each section was plotted as a histogram [*Gnaq*$^{d/d}$ ($n = 4$) and *Gnaq*$^{fl/fl}$ littermates ($n = 4$); Fig. 1*J*]. As expected, the highest number of GnRH-immunoreactive neurons was generally found at or near the OVLT, with fewer cells in sections rostral and caudal to the OVLT (Gill et al., 2008; Fig. 1*J*). Genotype (KO vs WT) had no significant effect on the total GnRH-immunoreactive cell counts ($p = 0.5033$, $F_{(16,102)} = 0.9619$; Fig. 1*K*). Furthermore, an analysis of the number of GnRH neuronal fibers that project to the median eminence was found to be similar between *Gnaq*$^{d/d}$ and *Gnaq*$^{fl/fl}$ littermates.

Overall, these findings suggest that *Gnaq*$^{d/d}$ mice could be used to determine the role of $G\alpha_{q/11}$ in regulating reproductive maturation and function at the level of the GnRH neuron. This was because *Cre* activity was detected in almost all GnRH neurons analyzed throughout early development; therefore, in young

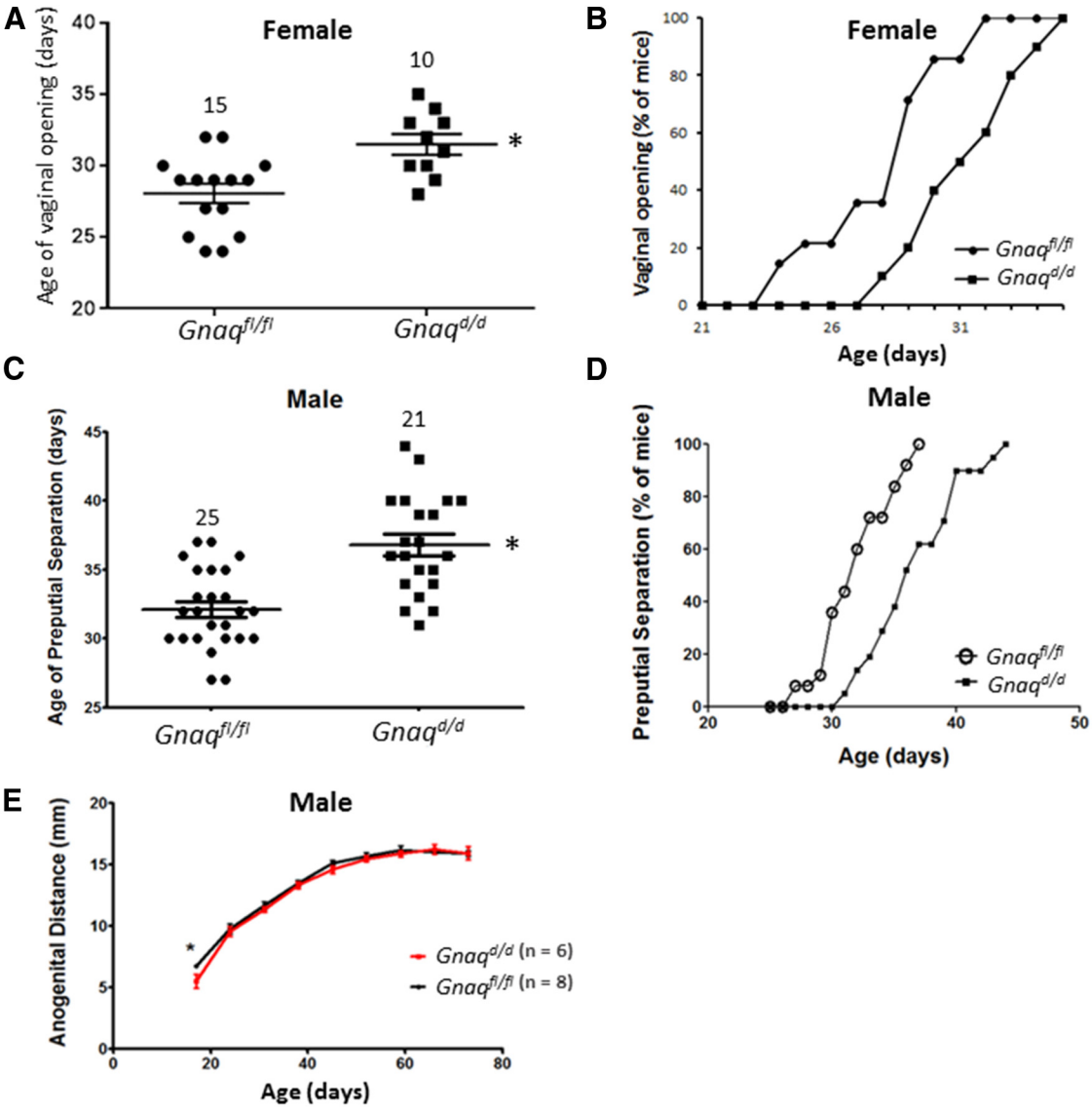

Figure 3. Reproductive maturation of *Gnaq*$^{fl/fl}$ and *Gnaq*$^{d/d}$ mice. Time course of day of vaginal opening (***A***, ***B***), preputial separation (***C***, ***D***), and anogenital distance development (***E***). Error bars represent SEM. *$p < 0.05$, significant difference.

adult mice we expect that $G\alpha_q$ would have been depleted in essentially all GnRH neurons. Additionally, in *Gnaq*$^{d/d}$ mice the GnRH neuronal population was fundamentally "intact," with detectable levels of GnRH in approximately the same number and distribution of immunoreactive neurons as in control mice.

Metabolic and reproductive profiling of *Gnaq*$^{d/d}$ mice

Total body weight is not affected in young pubertal Gnaq$^{d/d}$ *mice*

Since puberty in rodents is dependent on body weight (Frisch et al., 1985), the body weights of *Gnaq*$^{d/d}$ were determined by weighing mice frequently from P16 to P108 for females (Fig. 2*A*) and from P16 to P80 for males (Fig. 2*B*). For most of that time interval, which includes the peripubertal period, the loss of $G\alpha_{q/11}$ had no significant effect on body weight in both sexes ($p > 0.05$). However, at P16, *Gnaq*$^{fl/fl}$ control female and male mice were significantly heavier (female: $p = 0.036$, $t_{(33)} = 2.186$; male: $p = 0.0093$, $t_{(25)} = 2.82$) than their *Gnaq*$^{d/d}$ littermates (Fig. 2*A*,*B*), whereas at P100 and P108, this finding was reversed for females: *Gnaq*$^{d/d}$ mice were significantly heavier (P100: $p = 0.0153$, $t_{(11)} = 2.87$; P108: $p = 0.0137$, $t_{(2.931)} = 11$) than their *Gnaq*$^{fl/fl}$ littermates (Fig. 2*A*). The weights of males were only recorded up to P80, and up to this point in time, both *Gnaq*$^{d/d}$ and *Gnaq*$^{fl/fl}$ mice weighed the same (Fig. 2*B*).

Weights of the female reproductive tract and male testes are reduced in pubertal Gnaq$^{d/d}$ *mice*

Both gross examination and measurements of the weights of female reproductive tracts, expressed as a percentage of their total body weights, revealed that the reproductive tracts from 8- to 11-week-old *Gnaq*$^{d/d}$ females are ~67% smaller than those of littermate controls ($p < 0.0001$; Fig. 2*C*,*D*). Identical assessments revealed that testicular weights from unmated 8- to 11-week-old *Gnaq*$^{d/d}$ males were ~42% smaller than those of littermate controls ($p < 0.0001$; Fig. 2*C*,*D*). Thus, although total body weight was not different between experimental *Gnaq*$^{d/d}$ and control *Gnaq*$^{fl/fl}$ littermates from weeks 8 (P56) to 11 (P77), both female and male reproductive structures were significantly reduced in mass (Fig. 2).

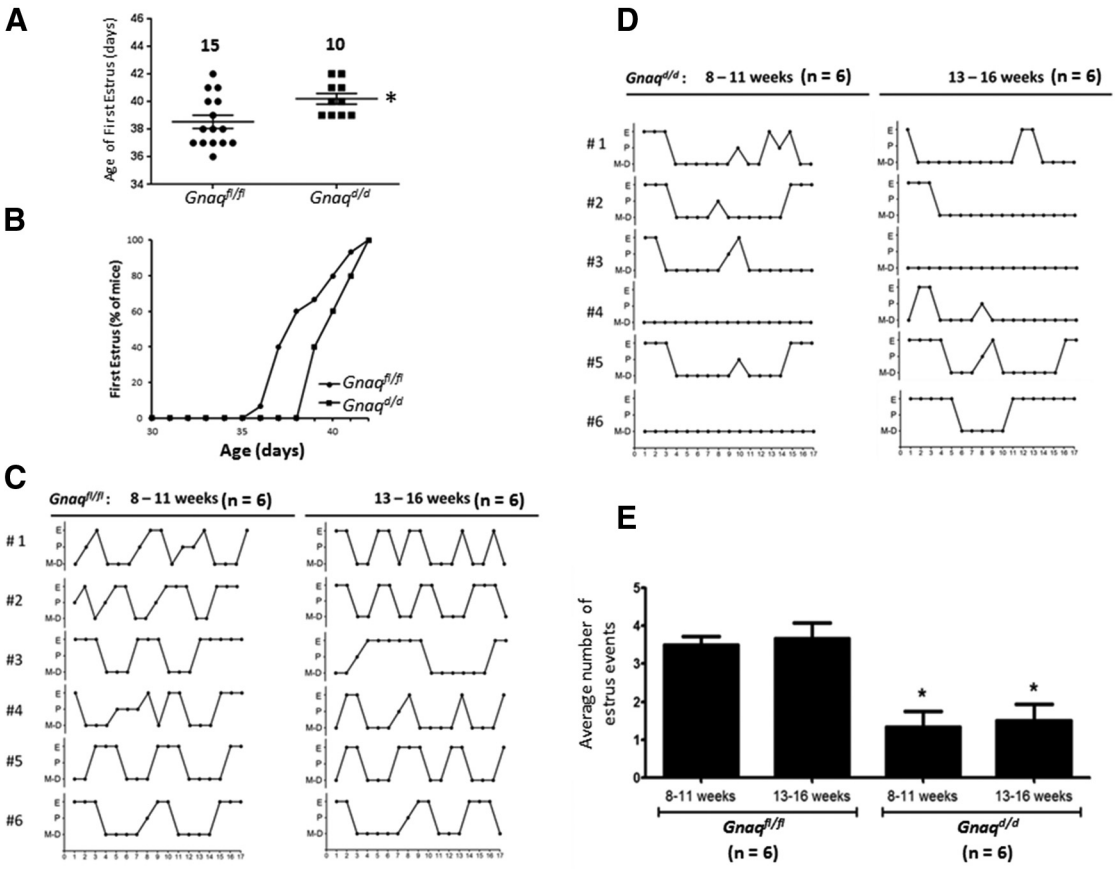

Figure 4. Estrous cycle staging of $Gnaq^{fl/fl}$ and $Gnaq^{d/d}$ female mice. ***A***, ***B***, Age at which first estrus is observed. ***C***, ***D***, Graphical representation of estrous staging (proestrus, estrus, or metestrus/diestrus) as determined for 17 d between 8:00 and 10:00 A.M. in 8- to 11-week-old females and again for another 17 d in the same females at 13–16 weeks of age. ***E***, The average number of times $Gnaq^{d/d}$ mice entered estrus during the two 17 d periods was compared with $Gnaq^{fl/fl}$ littermates using unpaired two-tailed *t* tests. Error bars represent SEM. $*p < 0.05$, significant difference.

Pubertal onset is delayed in $Gnaq^{d/d}$ *mice*

Pubertal onset was assessed in females by vaginal opening [defined as complete canalization of the vagina, it is an event that occurs with increased estrogen secretion (Nelson et al., 1982; Herbison et al., 2008; Caligioni, 2009) and in males by preputial separation and anogenital distance [events that reflect androgen exposure (Pakarainen et al., 2005; Lapatto et al., 2007; Novaira et al., 2014)]. Results show that vaginal opening ($p = 0.0027$, $t_{(23)} = 3.368$; Fig. 3*A*,*B*) and preputial separation ($p < 0.0001$, $t_{(44)} = 4.922$; Fig. 3*C*,*D*) were both significantly delayed. The delay in vaginal opening and preputial separation was not attributable to differences in body weights since there was no difference in weights in this time period for both female and male mice (Fig. 2). Interestingly, whereas preputial separation was delayed in $Gnaq^{d/d}$ males, anogenital distance was not affected except at P16 ($p = 0.0174$, $t_{(9)} = 2.906$; Fig. 3*E*), and this might reflect their higher body weight at P16 (Fig. 2*B*).

Gnaq$^{d/d}$ *female mice exhibit delayed first estrus and irregular estrous cycles that are characterized by fewer estrus events*

In addition to displaying delayed vaginal opening, first estrus was also significantly delayed in $Gnaq^{d/d}$ females ($p = 0.02$, $t_{(23)} = 2.5$; Fig. 4*A*,*B*). Based on estrous staging, control $Gnaq^{fl/fl}$ females exhibited an average cycle length of 5.2 ± 0.2 d ($n = 6$; Fig. 4*C*), whereas $Gnaq^{d/d}$ females exhibited highly irregular cycles that precluded cycle length calculation (Fig. 4*D*). Instead, the average number of times mice of a given genotype entered estrus was determined, and this revealed that $Gnaq^{d/d}$ mice entered estrus significantly fewer times than did control $Gnaq^{fl/fl}$ littermates ($p < 0.05$) and that the average number of mice that did this was similar between both age groups (Fig. 4*C*–*E*).

Gnaq$^{d/d}$ *female mice are anovulatory and therefore infertile*

To determine whether the estrus to diestrus transitions (Fig. 4*D*) were ovulatory, unmated $Gnaq^{d/d}$ mice were killed and their ovaries were examined histologically. Follicles at the primary, secondary, and early to mid-antral stages of development were present in $Gnaq^{d/d}$ mice, but there was no evidence of late antral (preovulatory or Graafian) follicles or corpora lutea (CL; Fig. 5*A*). In striking contrast, the ovaries of unmated $Gnaq^{fl/fl}$ females contained follicles at all stages of development and a large number of CL were also detected (Fig. 5*B*). Therefore, we concluded that even though $Gnaq^{d/d}$ mice transitioned from diestrus to estrus and back again, these "cycles" were anovulatory. Consistent with this observation, $Gnaq^{d/d}$ females ($n = 15$) failed to become pregnant when housed with a WT male of proven fertility (Fig. 5*C*). This finding led to the histological analysis of the uteri of $Gnaq^{d/d}$ females (Fig. 5*D*,*E*), and these were found to contain visibly fewer uterine glands relative to $Gnaq^{fl/fl}$ female littermates (Fig. 5*F*,*G*), a finding no doubt further associated with their infertility.

Gnaq$^{d/d}$ *male mice are subfertile and exhibit testicular phenotypes that vary from near normal to visibly mutant*

In contrast to the $Gnaq^{d/d}$ females, when $Gnaq^{d/d}$ males ($n = 15$) were individually housed with a WT female of proven fertility, 60% of the pairings (9 of 15) resulted in successful pregnancies and live births (Fig. 5*C*). The testes of fertile and infertile $Gnaq^{d/d}$

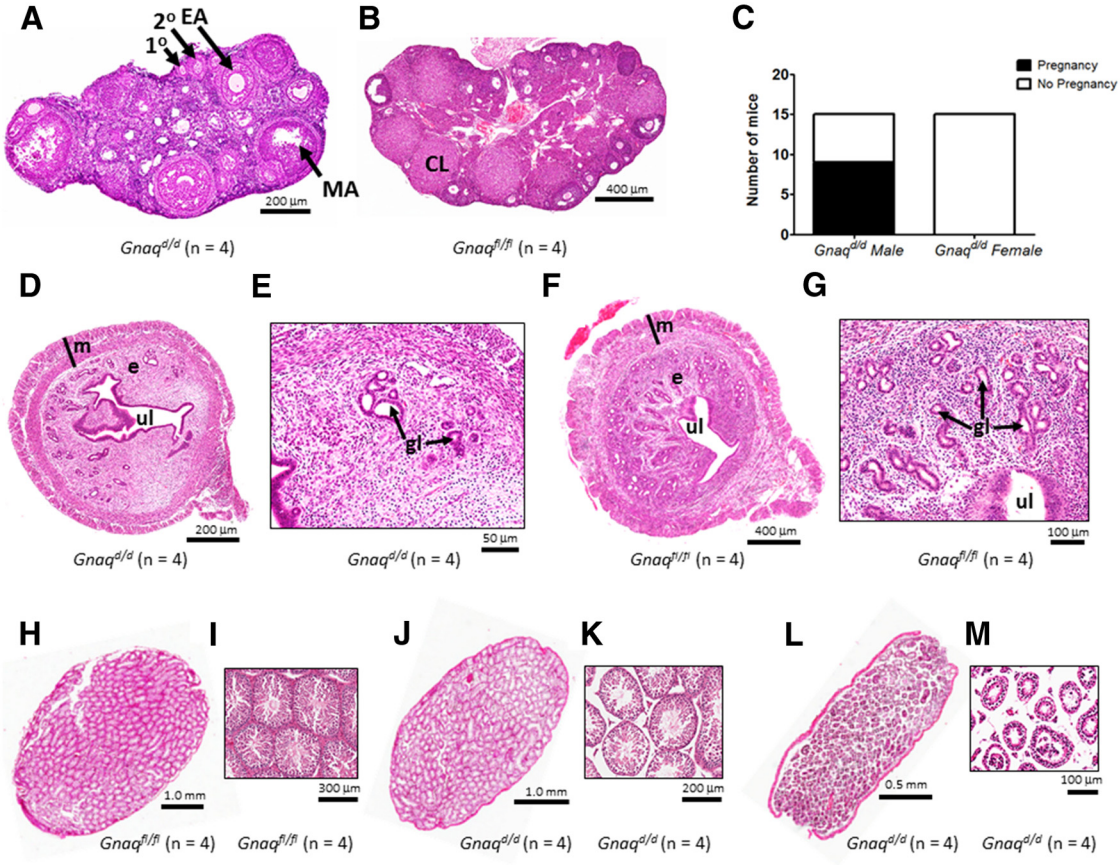

Figure 5. Gonadal histology of $Gnaq^{fl/fl}$ and $Gnaq^{d/d}$ mice. ***A***, ***B***, Representative sections of ovaries from $Gnaq^{d/d}$ and $Gnaq^{fl/fl}$ mice showing follicles at various stages of development, including primary (1°), pre-antral (2°), and early antral (EA) to mid-antral (MA); CL are also observed in the ovary from the $Gnaq^{fl/fl}$ mouse. ***C***, Fertility assessment of 15 female and male $Gnaq^{d/d}$ mice. ***D–G***, Representative sections of uteri from $Gnaq^{d/d}$ and $Gnaq^{fl/fl}$ mice showing the myometrium (m), endometrium (e), uterine lumen (ul), and uterine glands (g). Images shown in ***E*** and ***G*** are high-power magnifications of the endometrium from $Gnaq^{d/d}$ (***D***) and $Gnaq^{fl/fl}$ (***F***) mice, respectively. ***H–M***, Representative sections of testes from $Gnaq^{fl/fl}$ and $Gnaq^{d/d}$ mice showing the presence (***I***, ***K***) or absence (***M***) of spermatozoa in the seminiferous tubules. Testicular anatomy and spermatogenesis were variable in $Gnaq^{d/d}$ males (***J*** and ***K*** vs ***L*** and ***M***). Images shown in ***I***, ***K***, and ***M*** are high-power magnifications of the seminiferous tubules from testes shown in ***H***, ***J***, and ***L***, respectively.

males were subsequently analyzed histologically. Compared to fertile $Gnaq^{fl/fl}$ male littermates (Fig. 5*H*,*I*), fertile $Gnaq^{d/d}$ males displayed a similar number of seminiferous tubules, and although the tubules were not as tightly packed and evenly distributed as those seen in the central region of control testes, each tubule showed a well defined epithelium and clear evidence of a large number of developing sperm, based on the number of visible flagella (Fig. 5*J*,*K*). However, when compared with fertile $Gnaq^{fl/fl}$ and $Gnaq^{d/d}$ males (Fig. 5*H–K*), the testes of infertile $Gnaq^{d/d}$ male littermates exhibited less organized seminiferous tubules bearing few developing sperm, an observation again based on the number of visible flagella (Fig. 5*L*,*M*). These findings reveal that in $Gnaq^{d/d}$ males, testicular phenotypes ranged from almost normal to clearly mutant and these in turn gave rise to fertile and infertile $Gnaq^{d/d}$ males, respectively.

The HPG axis of $Gnaq^{d/d}$ mice exhibits significant hormonal responses to KP54 administration

Members of our research group have reported that KISS1R signals via both $G\alpha_{q/11}$- and β-arrestin-dependent (or $G\alpha_{q/11}$-independent) mechanisms (Pampillo et al., 2009; Szereszewski et al., 2010). It was further demonstrated that in mice lacking β-arrestin-1 or -2, KP54-triggered GnRH secretion was significantly diminished, as assessed indirectly by measuring serum gonadotropin levels (Ahow et al., 2014). Thus, we hypothesized that in mice lacking $G\alpha_{q/11}$ in their GnRH neurons ($Gnaq^{d/d}$), KP54 would continue to stimulate significant GnRH secretion, through $G\alpha_{q/11}$-independent mechanisms. This hypothesis was tested by quantifying serum hormone (FSH, LH, and testosterone) levels in KP54-stimulated versus saline-treated $Gnaq^{d/d}$ mice. All mice were 7-week-old virgins; females were ovariectomized, whereas males were used intact, and KP54 was administered intraperitoneally. First, we confirmed that KP54 (100 nmol KP54/kg body weight, 60 min) relative to saline would trigger a significant increase in hormone levels in $Gnaq^{fl/fl}$ littermate controls and found that it did (Fig. 6*A–E*). Next, we observed that in $Gnaq^{d/d}$ mice, KP54 also triggered a significant increase in hormone levels compared with saline treatment (Fig. 6*A–E*). These results support previous findings that Kiss1r can trigger GnRH secretion via $G\alpha_{q/11}$-independent pathways.

KP54-stimulated gonadotropin secretion in $Gnaq^{d/d}$ mice requires GnRH-R activation

Since the mouse pituitary expresses *Kiss1r* (for review, see Ahow et al., 2014), we tested whether the small but significant increase in KP54-stimulated hormone levels in $Gnaq^{d/d}$ mice was independent of GnRH secretion and GnRH-R activation and, instead, the result of peripherally administered KP54 acting directly on gonadotrope-expressed Kiss1r. To do so, for both male $Gnaq^{d/d}$ experimental and $Gnaq^{fl/fl}$ control littermates we measured

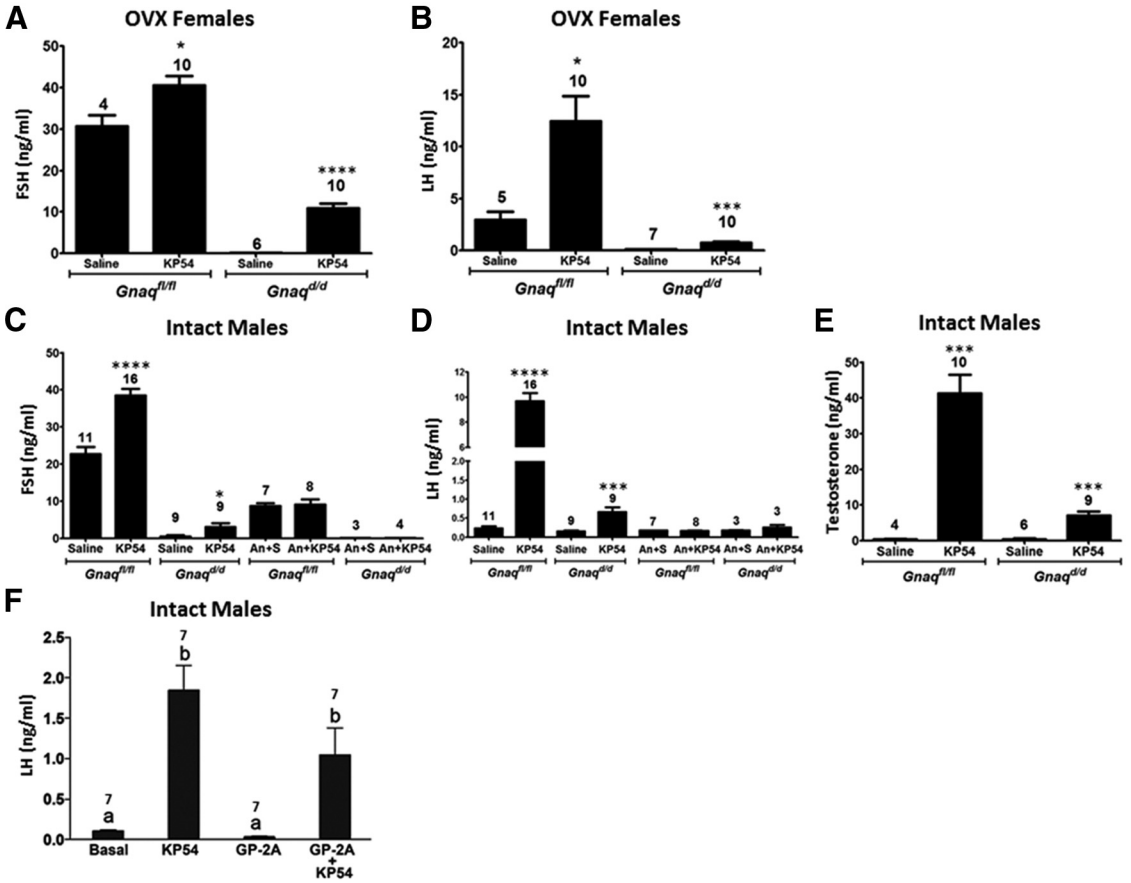

Figure 6. Serum hormonal responses to a KP54 challenge in *Gnaq*$^{fl/fl}$ and *Gnaq*$^{d/d}$ mice. ***A–E***, Serum FSH and LH levels, as well as testosterone levels in males only, were measured in 9-week-old virgin male and female *Gnaq*$^{d/d}$ and *Gnaq*$^{fl/fl}$ mice. Whereas intact males were used in this study, females were ovariectomized (OVX) 2 weeks before the KP54 challenge. Mice were administered either a single i.p. injection of 100 μl of vehicle (saline) or 100 μl of 100 nmol KP54/kg body weight. In a separate cohort of 9-week-old ovariectomized females and intact males, mice received two 100 μl, s.c. injections of the GnRH antagonist, Antide (1.25 μg/g body weight dissolved in sterile saline). Antide was administered at 24 and 1 h before i.p. injection of 100 μl of vehicle (saline) or 100 μl of 0.1 nmol KP54/g body weight. In all studies, 1 h after the KP54 injection, blood was collected by cardiac puncture. The number of mice used in these studies is indicated above each bar. An, Antide; S, saline. For ***A–E***, a given KP54 response was compared with its respective saline control response or a given An + KP54 response was compared with its respective An + saline control response. Data were analyzed by Student's *t* test where $p < 0.05$ was considered statistically significant. *$p < 0.05$, ***$p < 0.001$, ****$p < 0.0001$. Error bars represent SEM. ***F***, In another cohort of 12-week-old intact *Gnaq*$^{d/d}$ males ($n = 7$), mice were challenged through central injections with KP54 (100 pmol) or the Gαq inhibitor, GP2A (5 nmol) and blood was collected 30 min after. For the GP-2A + KP54 group, mice were injected 30 min apart and blood was collected 30 min after the KP54 injection. For ***F***, all treatments were compared with one another. Data were analyzed by two-way ANOVA followed by a Tukey *post hoc* test where different letters indicate significant differences between groups ($p < 0.05$). Error bars represent SEM.

KP54-triggered FSH and LH secretion relative to saline treatment in the presence and absence of the GnRH-R antagonist, Antide, and determined what effect Antide had on KP54-stimulated gonadotropin secretion for a given genotype. As reported above, regardless of genotype (*Gnaq*$^{fl/fl}$ or *Gnaq*$^{d/d}$), relative to saline treatment, KP54 (100 nmol KP54/kg body weight, 60 min) triggered a significant increase in hormone levels (Fig. 6*C*,*D*). However, this increase was fully blocked by Antide pretreatment ($p > 0.05$), not just in *Gnaq*$^{fl/fl}$ mice, but also in *Gnaq*$^{d/d}$ mice (Fig. 6*C*,*D*).

Together, these results (Fig. 6*A–E*) reveal that regardless of genotype, KP54-triggered gonadotropin secretion occurs entirely via GnRH-R and, therefore, KP54-stimulated hormone secretion in *Gnaq*$^{d/d}$ mice must occur through Kiss1r-coupled $G\alpha_{q/11}$-independent GnRH secretion by GnRH neurons.

KP54-triggered LH secretion in *Gnaq*$^{d/d}$ mice is not the result of differential GnRH-cre activity among the population of GnRH neurons

Although we demonstrated that GnRH-Cre was active in >98% of all GnRH neurons as early as E18 (Fig. 1*B–G*), we considered the possibility that *Gnaq*$^{fl/fl}$ escaped recombination in a few GnRH neurons and that this might account for the milder reproductive phenotype seen in the adult *Gnaq*$^{d/d}$ mice. To test whether this was likely, LH secretion was measured in male *Gnaq*$^{d/d}$ mice ($n = 7$) that were pretreated centrally with a peptide that is reported to potently antagonize $G\alpha_q$ signaling (Folkers et al., 1984; Hunt et al., 1999; Zoudilova et al., 2007; Najafi, 2009; Winter et al., 2011). The underlying idea was that the centrally administered drug would target all GnRH neurons and thereby block $G\alpha_q$ signaling in any neurons in which *Gnrh-Cre* was not expressed or in which Cre was not active. As expected, the results showed that in *Gnaq*$^{d/d}$ mice, centrally administered KP54, triggered a significant increase in LH secretion over untreated (basal) mice ($p = 0.0018$; $F_{(3,22)} = 18.21$; Fig. 6*F*). GP-2A had no measurable effect on basal LH secretion ($p > 0.05$) and was unable to significantly reduce KP54-stimulated LH secretion ($p > 0.05$; Fig. 6*F*). This leads us to conclude that KP54-triggered LH secretion observed in *Gnaq*$^{d/d}$ mice is not the result of $G\alpha_q$ signaling in the few neurons that lacked Cre activity.

Inactivation of *Gnaq* and *Gna11* diminished but did not ablate *Fshb* and *Lhb* expression in the pituitary

To further understand the impact of *Gnaq* as well as *Gna11* inactivation on gonadotropin levels, the expression of *Kiss1*, *Kiss1r*, *Gnrh1*, *Gnrhr1*, *Fshb*, and *Lhb* was assessed in $Gnaq^{d/d}$ male mice relative to WT males from the same parental strain (C57BL/6J). WT mice were used instead of $Gnaq^{fl/fl}$ littermate controls so that the effect of the combined inactivation of *Gnaq* and *Gna11* on gene expression could be determined. Our results revealed that inactivation of *Gnaq* and *Gna11* resulted in significantly increased hypothalamic *Kiss1* expression (Fig. 7*A*). Pituitary *Kiss1* expression was unaffected (Fig. 7*A*). Neither the inactivation of *Gnaq* and *Gna11* nor the increased expression of *Kiss1* had any effect on *Kiss1r* expression in the hypothalamus or pituitary (Fig. 7*B*). Like *Kiss1*, hypothalamic *Gnrh1* expression was also significantly elevated in $Gnaq^{d/d}$ mice (Fig. 7*C*). This was not surprising based on previous studies that reported kisspeptin, likely via the transcription factor Otx-2, positively regulates *Gnrh1* expression (Novaira et al., 2012). *Gnrh1* expression was not detected in the pituitary of both $Gnaq^{d/d}$ and WT mice (Fig. 7*C*). Despite an increase in hypothalamic *Gnrh1* expression, pituitary *Gnrhr1* levels decreased (Fig. 7*D*). Hypothalamic *Gnrhr1* expression was not detected in either $Gnaq^{d/d}$ or WT mice (Fig. 7*D*). Although *Gnrhr1* expression is positively regulated by GnRH (Kaiser et al., 1997), higher *Gnrh1* levels did not result in increased *Gnrhr1* expression in the pituitary (Fig. 7*C*,*D*), and this was likely due to the reduction in GnRH secretion in $Gnaq^{d/d}$ mice. The combined reduction in GnRH secretion and *Gnrhr1* levels would have resulted in diminished GnRH/GnRH-R signaling in the pituitary of $Gnaq^{d/d}$ mice and this would account for the significant reduction in pituitary *Fshb* and *Lhb* expression (Fig. 7*E*,*F*). Hypothalamic *Fshb* and *Lhb* expression was not detected in both $Gnaq^{d/d}$ and WT mice (Fig. 7*E*,*F*). Overall, as a result of the inactivation of *Gnaq* and *Gna11* in the GnRH neuron, there was no evidence of unexpected and compensatory changes in gene expression that could account for the continued, though diminished, kisspeptin-dependent gonadotropin secretion observed in $Gnaq^{d/d}$ mice.

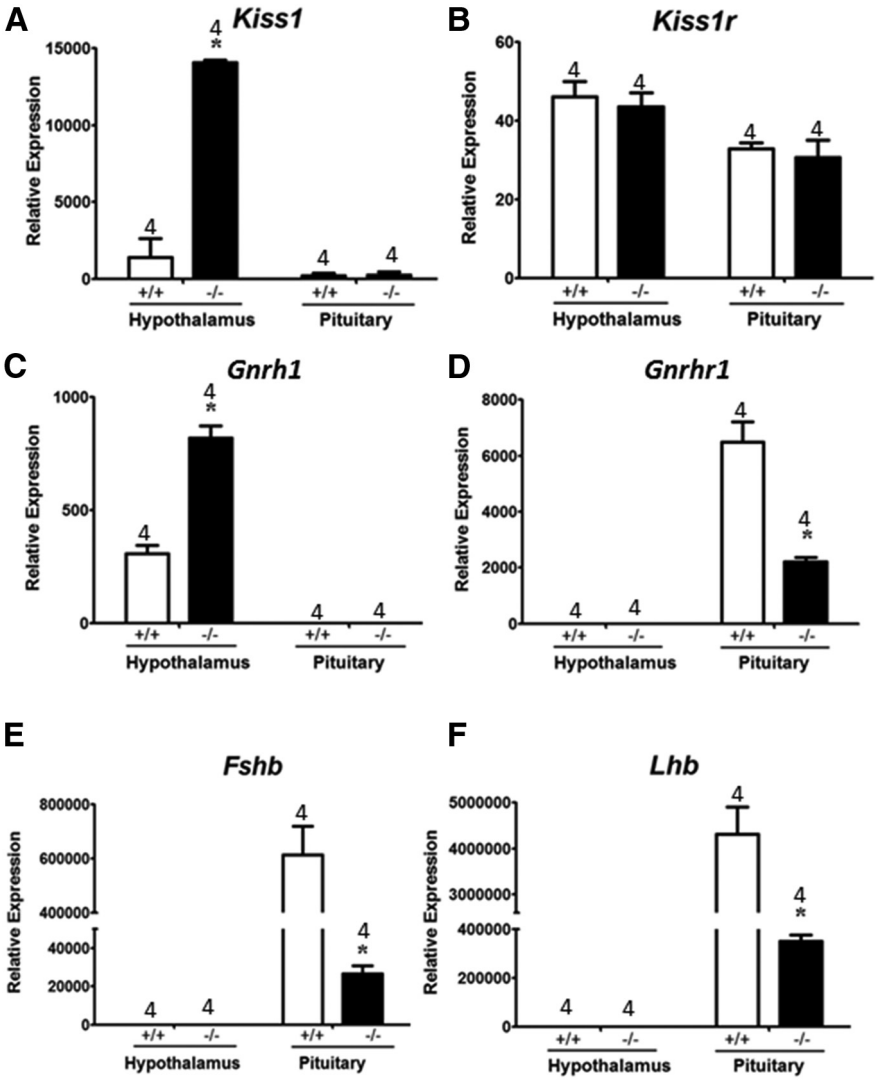

Figure 7. Quantitative real-time RT-PCR studies of gene expression in $Gnaq^{d/d}$ and $Gnaq^{fl/fl}$ mice. Gene expression data from the hypothalamus and pituitary of 8- to 9-week-old untreated and intact virgin male $Gnaq^{d/d}$ and $Gnaq^{fl/fl}$ mice. Gene expression was determined for *Kiss1* (***A***), *Kiss1r* (***B***), *Gnrh-1* (***C***), *Gnrh-r1* (***D***), *Fshb* (***E***), and *Lhb* (***F***). Gene expression was normalized to *Actb* expression and presented as relative expression. $*p < 0.05$, significant difference compared with $Gnaq^{fl/fl}$ mice.

A single dose of exogenous gonadotropins rescued follicular maturation and ovulation failure in $Gnaq^{d/d}$ mice

As reported earlier, whereas the ovaries of unmated $Gnaq^{fl/fl}$ females displayed several CL, the ovaries from unmated $Gnaq^{d/d}$ females did not; furthermore, follicular development stalled at the early to mid-antral stage of maturation (Fig. 5*A*,*B*). Thus, the ovaries of $Gnaq^{d/d}$ females appeared to be defective in late-stage follicular maturation and ovulation. Consistent with this, FSH ($p < 0.001$) and LH ($p < 0.01$) levels were also very low in ovariectomized saline-treated (nonstimulated) $Gnaq^{d/d}$ females compared with ovariectomized saline-treated $Gnaq^{fl/fl}$ females (Fig. 6*A*,*B*). To determine whether follicular maturation and ovulation could be rescued, $Gnaq^{d/d}$ female mice ($n = 4$) were superovulated and mated to WT males of proven fertility (D0). On the morning of D4, mice were killed and their uteri were excised and flushed to collect preimplantation embryos. Results showed that in all females examined, there was successful ovulation, based on the large number of CL detected in the ovaries and oocytes and embryos recovered from the uterine horns (Fig. 8). Despite successful ovulation, in only two of the four females were preimplantation embryos detected (Fig. 8*A*–*D*). In the other two females a large number of unfertilized oocytes ($n = 13, 23$) were detected (Fig. 8*E*–*H*).

Discussion

The GnRH neuron-specific *Kiss1r*-null mice ($Kiss1r^{d/d}$) and whole-body *Kiss1r*-null mouse ($Kiss1r^{-/-}$) exhibit hypogonadotropic hypogonadism and infertility and are unresponsive to a kisspeptin challenge (Seminara et al., 2003; Lapatto et al., 2007;

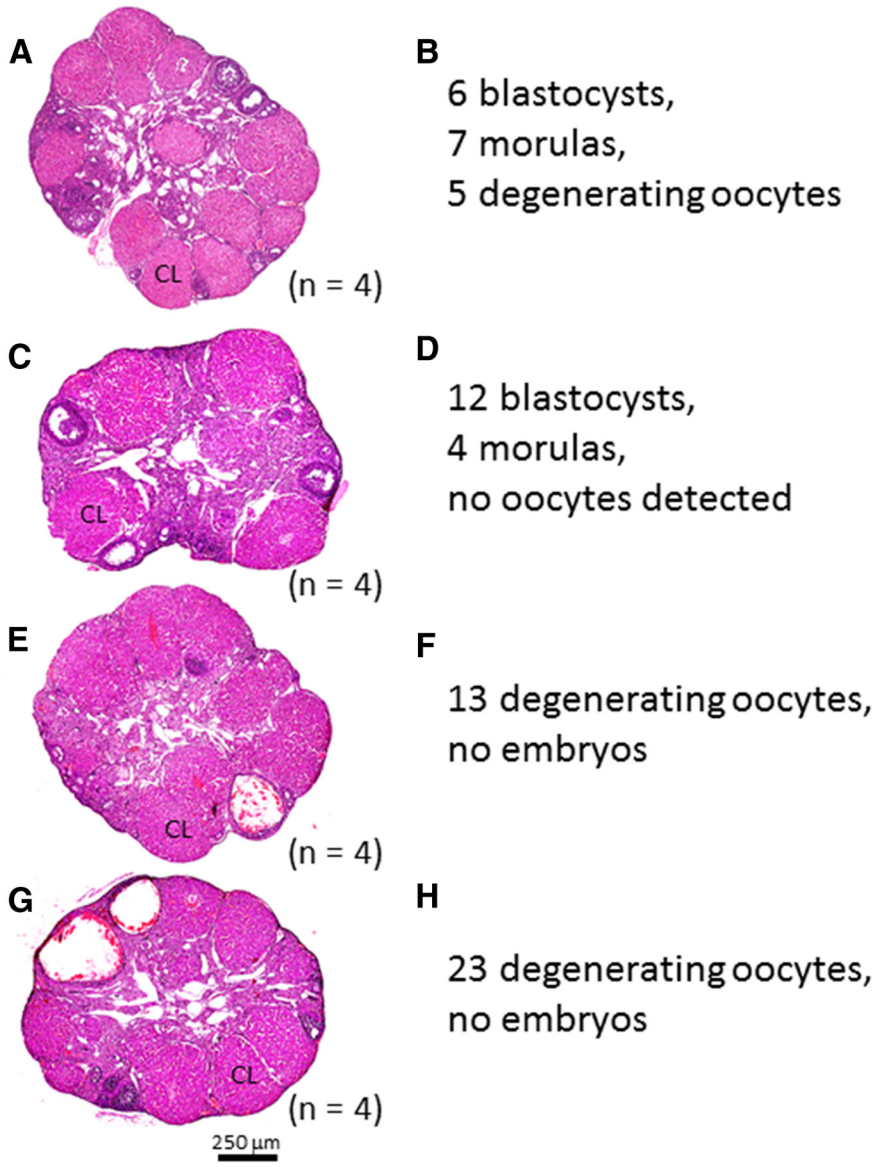

Figure 8. Superovulation of female *Gnaq*$^{d/d}$ mice and isolation and characterization of preimplantation embryos. Female *Gnaq*$^{d/d}$ mice, 6–8 weeks old, were superovulated and mated to WT males. ***A***, ***C***, ***E***, ***G***, Histological analysis of the ovaries confirms successful superovulation based on the abundance of corpora lutea. ***B***, ***D***, ***F***, ***H***, Unfertilized eggs and preimplantation embryos were collected from the uterus on D4 after mating and quantified and characterized.

Kirilov et al., 2013; Novaira et al., 2014). Here we report that inactivation of $G\alpha_{q/11}$ in the GnRH neuron affects reproductive maturation, but less so than in *Kiss1r*$^{d/d}$ and *Kiss1r*$^{-/-}$ mice. Thus, we conclude that in the absence of Kiss1r, KP-dependent GnRH secretion cannot occur; however, if Kiss1r is present and $G\alpha_q$ and $G\alpha_{11}$ are absent, Kiss1r will couple to $G\alpha_{q/11}$-independent pathways in the GnRH neuron to mediate KP-dependent GnRH secretion. This will be addressed further later in the discussion.

In *Kiss1r*$^{-/-}$ (129S1/SvImJ genetic background) and *Gnaq*$^{d/d}$ (C57BL/6J genetic background) mice, although the reduction in weights of the female reproductive tract was similar between the *Kiss1r*$^{-/-}$ (Lapatto et al., 2007) and *Gnaq*$^{d/d}$ (present data) female mice, the reduction in testicular weight in the *Kiss1r*$^{-/-}$ (Lapatto et al., 2007) and *Kiss1r*$^{d/d}$ (mixed CD1/129S1/SvImJ/C57BL/6J genetic background; Novaira et al., 2014) mice was approximately twice that of the *Gnaq*$^{d/d}$ mice. This suggests that the testes of *Gnaq*$^{d/d}$ mice are much less affected by $G\alpha_{q/11}$ inactivation at the level of the GnRH neuron than the testes of the whole-body *Kiss1r*$^{-/-}$ mice or GnRH neuron-specific *Kiss1r*$^{d/d}$ mice.

When other markers of reproductive maturation were assessed, vaginal opening in *Kiss1r*$^{-/-}$ and *Kiss1r*$^{d/d}$ females was more greatly delayed compared with *Gnaq*$^{d/d}$ females (Lapatto et al., 2007; Novaira et al., 2014). In *Kiss1r*$^{d/d}$ females (C57BL/6J genetic background; Kirilov et al., 2013) vaginal opening was not observed at all. Regarding preputial separation, although this was not measured in *Kiss1r*$^{-/-}$ males (Lapatto et al., 2007), it was detected in some *Kiss1r*$^{d/d}$ males and was delayed by ~9 d (Novaira et al., 2014); for *Gnaq*$^{d/d}$ it was detected in all males and delayed by ~5 d. As for anogenital distance, it was reduced in *Kiss1r*$^{-/-}$ males (Lapatto et al., 2007), whereas differences were generally not observed in *Gnaq*$^{d/d}$ males. Overall, the results reveal that reproductive maturation is less severely affected in *Gnaq*$^{d/d}$ mice compared with *Kiss1r*$^{-/-}$ and *Kiss1r*$^{d/d}$ mice.

Whereas *Kiss1r*$^{d/d}$ females (Kirilov et al., 2013; Novaira et al., 2014) were not observed to enter estrus, *Kiss1r*$^{-/-}$ females (129S1/SvImJ genetic background) first exhibited estrus at a median age of ~38 weeks, but transitions into and out of estrus were not associated with ovulation (Chan et al., 2009). *Gnaq*$^{d/d}$ females entered estrus as early as 6 weeks. Transitions into and out of estrus were also not associated with ovulation. Therefore, compared with *Kiss1r*$^{-/-}$ and *Kiss1r*$^{d/d}$ mice, disruption and age of onset of estrous cycles in *Gnaq*$^{d/d}$ mice is less severe, an observation that is consistent with previously discussed indicators of reproductive maturation.

When the seminiferous tubules of *Kiss1r*$^{-/-}$ and *Kiss1r*$^{d/d}$ males were examined, several phenotypes were described. For *Kiss1r*$^{-/-}$ males, varying degrees of spermatogenesis were observed, ranging from arrested to full development (Lapatto et al., 2007; Chan et al., 2009). For *Kiss1r*$^{d/d}$ males, spermatozoa were either not detected (Kirilov et al., 2013) or detected at reduced numbers (Novaira et al., 2014). Like *Kiss1r*$^{-/-}$ males, *Gnaq*$^{d/d}$ males also displayed varying degrees of spermatogenesis. In fertility experiments, Lapatto et al. (2007) reported that when *Kiss1r*$^{-/-}$ males were housed with WT females of proven fertility, there were no pregnancies. This is not surprising given that these males did not show preputial separation. In similar studies (Kirilov et al., 2013; Novaira et al., 2014), others have reported that when *Kiss1r*$^{d/d}$ males that showed preputial separation were housed with WT females of proven fertility, there were still no pregnancies. For *Gnaq*$^{d/d}$ males, pairings involving males with preputial separation resulted in successful pregnancies and live birth. This again reveals that the reproductive phenotype is less severe in *Gnaq*$^{d/d}$ mice.

In the study by Lapatto et al. (2007) using *Kiss1r*$^{-/-}$ mice, kisspeptin stimulation (non-gonadectomized mice, 50 nmol KP10, i.p., 30 min) failed to trigger changes in basal gonadotropin levels. In the study by Novaira et al. (2014) using *Kiss1r*$^{d/d}$ mice, kisspeptin stimulation (non-gonadectomized mice, 1 nmol KP10, i.p., 10 min) also failed to elicit FSH and LH responses. For *Gnaq*$^{d/d}$ mice, however, kisspeptin stimulation (non-gonadectomized males and ovariectomized females, 100 nmol KP54/kg body weight or 2 nmol/20 g mouse, i.p., 60 min) triggered a significant increase in gonadotropin and testosterone levels. Furthermore, the $G\alpha_q$ inhibitor, GP-2A, was unable to block the KP54-triggered increase in LH in *Gnaq*$^{d/d}$ males (non-gonadectomized males, 100 pmol/5 μl, i.c.v., 30 min). Although the three studies cannot be compared directly to each other due to differences in experimental protocols, there is sufficient evidence to suggest that *Gnaq*$^{d/d}$ mice exhibit Kiss1r-coupled $G\alpha_{q/11}$-independent signaling and that this underlies the kisspeptin-dependent gonadotropin and testosterone responsiveness not seen in *Kiss1r*$^{-/-}$ and *Kiss1r*$^{d/d}$ mice.

Based on the efficiency of *Gnrh-Cre*-mediated GFP expression in the *ROSA26-loxP-stop-loxP-GFP* reporter line, the observation that the $G\alpha_q$ inhibitor, GP-2A, could not significantly block KP54-triggered LH secretion in *Gnaq*$^{d/d}$ mice and the absence of compensatory changes in gene expression within the neuroendocrine axis of *Gnaq*$^{d/d}$ mice, we conclude that the milder reproductive phenotypes observed in *Gnaq*$^{d/d}$ mice must reflect $G\alpha_{q/11}$-independent signaling at the level of the GnRH neuron. It is interesting to note that in their recent study, Kirilov et al. (2013) used the identical *Gnrh-Cre* line (Yoon et al., 2005) used in this study, and the conditional inactivation of *Kiss1r* triggered severe hypogonadal phenotypes; in striking contrast, milder phenotypes were observed in the *Gnaq*$^{d/d}$ mice. Together, not only do these findings strengthen the conclusion that Cre activity was efficient and widespread among the GnRH neuronal population, but, again, the milder reproductive phenotypes observed in *Gnaq*$^{d/d}$ mice must reflect $G\alpha_{q/11}$-independent GnRH secretion and activation of the neuroendocrine-reproductive axis. Furthermore, since ablation of $G\alpha_{q/11}$ in GnRH neurons would eliminate $G\alpha_{q/11}$-mediated signaling by all $G\alpha_{q/11}$-coupled receptors, including those involved in stimulating GnRH secretion in response to other hormones and neuropeptides (Todman et al., 2005), *Gnaq*$^{d/d}$ mice might be expected to exhibit even more severe phenotypes than *Kiss1r*$^{d/d}$ mice. However, this was not observed, making the less severe phenotypes all the more supportive of $G\alpha_{q/11}$-independent signaling.

Overall, our data strongly suggest that in the absence of $G\alpha_{q/11}$ in GnRH neurons, Kiss1r remains signaling competent. We first considered that this occurs via other G-proteins. However, it was reported that Kiss1r does not signal via $G\alpha_s$ and $G\alpha_{i/o}$ (Kotani et al., 2001; Muir et al., 2001) and among the remaining $G\alpha_q$ family members [$G\alpha_{14}$ and $G\alpha_{15}$ (mouse)/16 (human)], whereas Kiss1r can signal via $G\alpha_{15/16}$ (Kotani et al., 2001; Wacker et al., 2008), it does not appear to do so via $G\alpha_{14}$ (A. Babwah, unpublished observations). Furthermore, given that $G\alpha_{14}$ and $G\alpha_{15}$ are not expressed in the mouse hypothalamus (for review, see Millar and Babwah, 2015), it is unlikely that Kiss1r signals via other G-proteins in the wild-type mouse. It is possible, though, that loss of $G\alpha_{q/11}$ in GnRH neurons triggers compensatory signaling, for example, by upregulating $G\alpha_{15/16}$ expression, by coupling Kiss1r to both G-protein and non-G-protein pathways that Kiss1r would not normally couple to under normal conditions such that these pathways become more physiologically relevant in the absence of $G\alpha_{q/11}$ signaling or even through the activation of Kiss1r in non-GnRH neuronal cells such as the preoptic nNOS neuronal population (Hanchate et al., 2012). However, given the scattered distribution of GnRH neurons in the hypothalamus, the technical difficulty in isolating pure populations of GnRH neurons and the lack of robust antibodies against Gαq family members, we could not confidently address that possibility through the analysis of either mRNA or protein expression.

We have also considered that part of the KP-dependent GnRH/LH secretion observed in the conditional *Gnaq*$^{d/d}$ mice might still be occurring via $G\alpha_{q/11}$, but through the preoptic nNOS neuronal population, which is morphologically associated with kisspeptin fibers and express Kiss1r (Hanchate et al., 2012). This population of neurons has been demonstrated to regulate both tonic pulsatile and KP-dependent surge release of GnRH/LH in the female mouse (Hanchate et al., 2012). It is likely that if the nNOS neuronal population accounts for all or part of the observed KP-stimulated GnRH/LH secretion in the *Gnaq*$^{d/d}$ mice, it might be a female-specific phenomenon since Navarro et al. (2005) reported that in male rats, pharmacological inhibition of nNOS failed to alter basal or KP-triggered LH release. Although failure to observe signaling via the nNOS neuronal population might reflect sex differences in KP-stimulated LH release (Jayasena et al., 2011), the underlying reason might be more complex since Novaira et al. (2014) did not observe KP-dependent LH release in both male and female mice bearing a conditional deletion of *Kiss1r* in their GnRH neurons.

In conclusion, the persistent responsiveness to KP54 suggests that kisspeptin signals through $G\alpha_{q/11}$-independent pathways at the level of the GnRH neuron and that such signaling is physiologically relevant since some males can achieve fertility without intervention and females, while infertile, respond efficiently to exogenous gonadotropins and can subsequently undergo spontaneous pregnancy.

References

Ahow M, Min L, Pampillo M, Nash C, Wen J, Soltis K, Carroll RS, Glidewell-Kenney CA, Mellon PL, Bhattacharya M, Tobet SA, Kaiser UB, Babwah AV (2014) KISS1R signals independently of $G\alpha_{q/11}$ and triggers LH secretion via the beta-arrestin pathway in the male mouse. Endocrinology 155:4433–4446. CrossRef Medline

Calder M, Chan YM, Raj R, Pampillo M, Elbert A, Noonan M, Gillio-Meina C, Caligioni C, Bérubé NG, Bhattacharya M, Watson AJ, Seminara SB, Babwah AV (2014) Implantation failure in female *Kiss1*$^{-/-}$ mice is independent of their hypogonadic state and can be partially rescued by leukemia inhibitory factor. Endocrinology 155:3065–3078. CrossRef Medline

Caligioni CS (2009) Assessing Reproductive Status/Stages in Mice. Curr Protoc Neurosci July:Appendix 4:Appendix 4I. CrossRef Medline

Chan YM, Broder-Fingert S, Wong KM, Seminara SB (2009) Kisspeptin/Gpr54-independent gonadotrophin-releasing hormone activity in *Kiss1* and *Gpr54* mutant mice. J Neuroendocrinol 21:1015–1023. CrossRef Medline

de Roux N, Genin E, Carel JC, Matsuda F, Chaussain JL, Milgrom E (2003) Hypogonadotropic hypogonadism due to loss of function of the KiSS1-derived peptide receptor KISS1R. Proc Natl Acad Sci U S A 100:10972–10976. CrossRef Medline

Dettlaff-Swiercz DA, Wettschureck N, Moers A, Huber K, Offermanns S (2005) Characteristic defects in neural crest cell-specific Galphaq/Galpha11- and Galpha12/Galpha13-deficient mice. Dev Biol 282:174–182. CrossRef Medline

Druckenbrod NR, Epstein ML (2005) The pattern of neural crest advance in the cecum and colon. Dev Biol 287:125–133. CrossRef Medline

Ellinwood WE, Ronnekleiv OK, Kelly MJ, Resko JA (1985) A new antiserum with conformational specificity for LHRH: usefulness for radioimmunoassay and immunocytochemistry. Peptides 6:45–52. CrossRef Medline

Folkers K, Håkanson R, Hörig J, Xu JC, Leander S (1984) Biological evaluation of substance P antagonists. Br J Pharmacol 83:449–456. CrossRef Medline

Frisch RE (1985) Fatness, menarche, and female fertility. Perspect Biol Med 28:611–633. CrossRef Medline

Funes S, Hedrick JA, Vassileva G, Markowitz L, Abbondanzo S, Golovko A, Yang S, Monsma FJ, Gustafson EL (2003) The KiSS-1 receptor GPR54 is essential for the development of the murine reproductive system. Biochem Biophys Res Commun 312:1357–1363. CrossRef Medline

Gaytan F, Bellido C, Aguilar R, Aguilar E (1988) Balano-preputial separation as an external sign of puberty in the rat: correlation with histologic testicular data. Andrologia 20:450–453. Medline

Gill JC, Wadas B, Chen P, Portillo W, Reyna A, Jorgensen E, Mani S, Schwarting GA, Moenter SM, Tobet S, Kaiser UB (2008) The gonadotropin-releasing hormone (GnRH) neuronal population is normal in size and distribution in GnRH-deficient and GnRH receptor-mutant hypogonadal mice. Endocrinology 149:4596–4604. CrossRef Medline

Hanchate NK, Parkash J, Bellefontaine N, Mazur D, Colledge WH, d'Anglemont de Tassigny X, Prevot V (2012) Kisspeptin-GPR54 signaling in mouse NO-synthesizing neurons participates in the hypothalamic control of ovulation. J Neurosci 32:932–945. CrossRef Medline

Herbison AE, Porteous R, Pape JR, Mora JM, Hurst PR (2008) Gonadotropin-releasing hormone neuron requirements for puberty, ovulation, and fertility. Endocrinology 149:597–604. CrossRef Medline

Hunt RA, Bhat GJ, Baker KM (1999) Angiotensin II-stimulated induction of sis-inducing factor is mediated by pertussis toxin-insensitive Gq proteins in cardiac myocytes. Hypertension 34:603–608. CrossRef Medline

Jayasena CN, Nijher GM, Comninos AN, Abbara A, Januszewki A, Vaal ML, Sriskandarajah L, Murphy KG, Farzad Z, MA Ghatei, Bloom SR, Dhillo WS (2011) The effects of kisspepetin-10 on reproductive hormone release show sexual dimorphism in humans. J Clin Endocrinol Metab 96: E1963–E1972. CrossRef Medline

Kaiser UB, Jakubowiak A, Steinberger A, Chin WW (1997) Differential effects of gonadotropin-releasing hormone (GnRH) pulse frequency on gonadotropin subunit and GnRH receptor messenger ribonucleic acid levels *in vitro*. Endocrinology 138:1224–1231. CrossRef Medline

Kirilov M, Clarkson J, Liu X, Roa J, Campos P, Porteous R, Schütz G, Herbison AE (2013) Dependence of fertility on kisspeptin-Gpr54 signaling at the GnRH neuron. Nat Commun 4:2492. CrossRef Medline

Kotani M, Detheux M, Vandenbogaerde A, Communi D, Vanderwinden JM, Le Poul E, Brézillon S, Tyldesley R, Suarez-Huerta N, Vandeput F, Blanpain C, Schiffmann SN, Vassart G, Parmentier M (2001) The metastasis suppressor gene KiSS-1 encodes kisspeptins, the natural ligands of the orphan G protein-coupled receptor KISS1R. J Biol Chem 276:34631–34636. CrossRef Medline

Lapatto R, Pallais JC, Zhang D, Chan YM, Mahan A, Cerrato F, Le WW, Hoffman GE, Seminara SB (2007) Kiss1$^{-/-}$ mice exhibit more variable hypogonadism than Gpr54$^{-/-}$ mice. Endocrinology 148:4927–4936. CrossRef Medline

Liu X, Lee K, Herbison AE (2008) Kisspeptin excites gonadotropin-releasing hormone neurons through a phospholipase C/calcium-dependent pathway regulating multiple ion channels. Endocrinology 149: 4605–4614. CrossRef Medline

Luque RM, Kineman RD, Tena-Sempere M (2007) Regulation of hypothalamic expression of KiSS-1 and GPR54 genes by metabolic factors: analyses using mouse models and a cell line. Endocrinology 148:4601–4611. CrossRef Medline

Mao X, Fujiwara Y, Chapdelaine A, Yang H, Orkin SH (2001) Activation of EGFP expression by cre-mediated excision in a new ROSA26 reporter mouse strain. Blood 97:324–326. CrossRef Medline

Martin C, Navarro VM, Simavli S, Vong L, Carroll RS, Lowell BB, Kaiser UB (2014) Leptin-responsive GABAergic neurons regulate fertility through pathways that result in reduced kisspeptinergic tone. J Neurosci 34:6047–6056. CrossRef Medline

Millar RP, Babwah AV (2015) KISS1R: hallmarks of an effective regulator of the neuroendocrine axis. Neuroendocrinology 101:193–210. CrossRef Medline

Muir AI, Chamberlain L, Elshourbagy NA, Michalovich D, Moore DJ, Calamari A, Szekeres PG, Sarau HM, Chambers JK, Murdock P, Steplewski K, Shabon U, Miller JE, Middleton SE, Darker JG, Larminie CG, Wilson S, Bergsma DJ, Emson P, Faull R, et al. (2001) AXOR12, a novel human G protein-coupled receptor, activated by the peptide KiSS-1. J Biol Chem 276:28969–28975. CrossRef Medline

Najafi SM (2009) Activators of G proteins inhibit GSK-3beta and stabilize beta-Catenin in *Xenopus* oocytes. Biochem Biophys Res Commun 382: 365–369. CrossRef Medline

Navarro VM, Castellano JM, Fernández-Fernández R, Tovar S, Roa J, Mayen A, Nogueiras R, Vazquez MJ, Barreiro ML, Magni P, Aguilar E, Dieguez C, Pinilla L, Tena-Sempere M (2005) Characterization of the potent luteinizing hormone-releasing activity of KiSS-1 peptide, the natural ligand of GPR54. Endocrinology 146:156–163. CrossRef Medline

Navarro VM, Bosch MA, León S, Simavli S, True C, Pinilla L, Carroll RS, Seminara SB, Tena-Sempere M, Rønnekleiv OK, Kaiser UB (2015) The integrated hypothalamic tachykinin-kisspeptin system as a central coordinator for reproduction. Endocrinology 156:627–637. CrossRef Medline

Nelson JF, Felicio LS, Randall PK, Sims C, Finch CE (1982) A longitudinal study of estrous cyclicity in aging C57BL/6J mice. I. Cycle frequency, length and vaginal cytology. Biol Reprod 27:327–339. CrossRef Medline

Novaira HJ, Fadoju D, Diaczok D, Radovick S (2012) Genetic mechanisms mediating kisspeptin regulation of GnRH gene expression. J Neurosci 32:17391–17400. CrossRef Medline

Novaira HJ, Sonko ML, Hoffman G, Koo Y, Ko C, Wolfe A, Radovick S (2014) Disrupted kisspeptin signaling in GnRH neurons leads to hypogonadotrophic hypogonadism. Mol Endocrinol 28:225–238. CrossRef Medline

Offermanns S, Hashimoto K, Watanabe M, Sun W, Kurihara H, Thompson RF, Inoue Y, Kano M, Simon MI (1997a) Impaired motor coordination and persistent multiple climbing fiber innervation of cerebellar Purkinje cells in mice lacking Gaq. Proc Natl Acad Sci U S A 94:14089–14094. CrossRef Medline

Offermanns S, Toombs CF, Hu YH, Simon MI (1997b) Defective platelet activation in Gaq deficient mice. Nature 389:183–186. CrossRef Medline

Offermanns S, Zhao LP, Gohla A, Sarosi I, Simon MI, Wilkie TM (1998) Embryonic cardiomyocyte hypoplasia and craniofacial defects in Gαq/Gα11-mutant mice. EMBO J 17:4304–4312. CrossRef Medline

Ohtaki T, Shintani Y, Honda S, Matsumoto H, Hori A, Kanehashi K, Terao Y, Kumano S, Takatsu Y, Masuda Y, Ishibashi Y, Watanabe T, Asada M, Yamada T, Suenaga M, Kitada C, Usuki S, Kurokawa T, Onda H, Nishimura O, et al. (2001) Metastasis suppressor gene KiSS-1 encodes peptide ligand of a G-protein-coupled receptor. Nature 411:613–617. CrossRef Medline

Pakarainen T, Zhang FP, Mäkelä S, Poutanen M, Huhtaniemi I (2005) Testosterone replacement therapy induces spermatogenesis and partially restores fertility in luteinizing hormone receptor knock-out mice. Endocrinology 146:596–606. CrossRef Medline

Pampillo M, Camuso N, Taylor JE, Szereszewski JM, Ahow MR, Zajac M, Millar RP, Bhattacharya M, Babwah AV (2009) Regulation of GPR54 signaling by GRK2 and β-arrestin. Mol Endocrinol 23:2060–2074. CrossRef Medline

Pau KYF, Orstead KM, Hess DL, Spies HG (1986) Feedback effects of ovarian steroids on the hypothalamic-hypophyseal axis in the rabbit. Biol Reprod 3:1009–1023.

Pfaffl MW (2001) A new mathematical model for relative quantification in real-time RT-PCR. Nucleic Acids Res 29:e45. CrossRef Medline

Rasmussen LE, Buss IO, Hess DL, Schmidt MJ (1984) Testosterone and dihydrotestosterone concentrations in elephant serum and temporal gland secretions. Biol Reprod 30:352–362. CrossRef Medline

Seminara SB, Messager S, Chatzidaki EE, Thresher RR, Acierno JS Jr, Shagoury JK, Bo-Abbas Y, Kuohung W, Schwinof KM, Hendrick AG, Zahn D, Dixon J, Kaiser UB, Slaugenhaupt SA, Gusella JF, O'Rahilly S, Carlton MB, Crowley WF Jr, Aparicio SA, Colledge WH (2003) The GPR54 gene as a regulator of puberty. N Engl J Med 349:1614–1627. CrossRef Medline

Singh SP, Wolfe A, Ng Y, DiVall SA, Buggs C, Levine JE, Wondisford FE, Radovick S (2009) Impaired estrogen feedback and infertility in female mice with pituitary-specific deletion of estrogen receptor alpha (ESR1). Biol Reprod 81:488–496. CrossRef Medline

Skynner MJ, Slater R, Sim JA, Allen ND, Herbison AE (1999) Promoter transgenics reveal multiple gonadotropin-releasing hormone-I-expressing cell populations of different embryological origin in mouse brain. J Neurosci 19:5955–5966. Medline

Strathmann M, Simon MI (1990) G protein diversity: a distinct class of alpha subunits is present in vertebrates and invertebrates. Proc Natl Acad Sci U S A 87:9113–9117. CrossRef Medline

Ström JO, Theodorsson A, Ingberg E, Isaksson IM, Theodorsson E (2012) Ovariectomy and 17β-estradiol replacement in rats and mice: a visual demonstration. J Vis Exp 64:e4013. CrossRef Medline

Szereszewski JM, Pampillo M, Ahow MR, Offermanns S, Bhattacharya M, Babwah AV (2010) GPR54 regulates ERK1/2 activity and hypothalamic gene expression in a Gαq/11 and β-arrestin-dependent manner. PLoS One 5:e12964. CrossRef Medline

Todman MG, Han SK, Herbison AE (2005) Profiling neurotransmitter receptor expression in mouse gonadotropin-releasing hormone neurons using green fluorescent protein-promoter transgenics and microarrays. Neurosci 132:703–712. CrossRef

Urbanski HF, Kim SO, Connolly ML (1990) The influence of photoperiod and 6-methoxybenzoxazolinone on the reproductive axis of inbred LSH/Ss Lak male hamsters. J Reprod Fert 90:157–163. CrossRef

Wacker JL, Feller DB, Tang XB, Defino MC, Namkung Y, Lyssand JS, Mhyre AJ, Tan X, Jensen JB, Hague C (2008) Disease-causing mutation in GPR54 reveals the importance of the second intracellular loop for class A G-protein-coupled receptor function. J Biol Chem 283:31068–31078. CrossRef Medline

Wettschureck N, Rütten H, Zywietz A, Gehring D, Wilkie TM, Chen J, Chien KR, Offermanns S (2001) Absence of pressure overload induced myocardial hypertrophy after conditional inactivation of Gα_q/Gα_{11} in cardiomyocytes. Nat Med 7:1236–1240. CrossRef Medline

White AC, Lavine KJ, Ornitz DM (2007) FGF9 and SHH regulate mesenchymal Vegfa expression and development of the pulmonary capillary network. Development 134:3743–3752. CrossRef Medline

Winter C, Kampik NB, Vedovelli L, Rothenberger F, Paunescu TG, Stehberger PA, Brown D, John H, Wagner CA (2011) Aldosterone stimulates vacuolar H^+-ATPase activity in renal acid-secretory intercalated cells mainly via a protein kinase C-dependent pathway. Am J Physiol Cell Physiol 301:C1251–C1261. CrossRef Medline

Wintermantel TM, Campbell RE, Porteous R, Bock D, Gröne HJ, Todman MG, Korach KS, Greiner E, Pérez CA, Schütz G, Herbison AE (2006) Definition of estrogen receptor pathway critical for estrogen positive feedback to gonadotropin-releasing hormone neurons and fertility. Neuron 52:271–280. CrossRef Medline

Wolfe A, Divall S, Singh SP, Nikrodhanond AA, Baria AT, Le WW, Hoffman GE, Radovick S (2008) Temporal and spatial regulation of CRE recombinase expression in gonadotrophin-releasing hormone neurones in the mouse. J Neuroendocrinol 20:909–916. CrossRef Medline

Wong ML, Medrano JF (2005) Real-time PCR for mRNA quantitation. Biotechniques 39:75–85. CrossRef Medline

Yoon H, Enquist LW, Dulac C (2005) Olfactory inputs to hypothalamic neurons controlling reproduction and fertility. Cell 123:669–682. CrossRef Medline

Zhang C, Bosch MA, Rønnekleiv OK, Kelly MJ (2013) Kisspeptin activation of TRPC4 channels in female GnRH neurons requires PIP2 depletion and cSrc kinase activation. Endocrinology 154:2772–2783. CrossRef Medline

Zoudilova M, Kumar P, Ge L, Wang P, Bokoch GM, DeFea KA (2007) β-Arrestin-dependent regulation of the cofilin pathway downstream of protease-activated receptor-2. J Biol Chem 282:20634–22646. CrossRef Medline